Universidad del País Vasco/Euskal Herriko Unibertsitatea
Facultad de Ciencias Químicas/Kimika Zientzien Fakultatea

Degree in chemistry:

BACHELOR FINAL PROJECT:

Synthesis and Characterization of Side-chain Cholesterol Based Linear Liquid Crystal Polyurethanes

Author: Aitor Hernández Toribio

Supervisors: Haritz Sardon – Jaime Martín

GIPUZKOAKO CAMPUSA - CAMPUS DE GIPUZKOA

Pº. Manuel de Lardizabal, 3 20018

San Sebastián, September of 2018

ABSTRACT:

Liquid crystal polymers (LCPs) are currently one of the most studied polymeric materials developed for new optical and photonic technology. The exclusive properties displayed by LCPs initiated a new research trend in polymer chemistry that has led to a wide range of specialized and daily use devices. On the other hand, the rising relevance of cholesterol based polymers in biotechnological applications in drug delivery, encouraged the study of the confluence point of the biotechnological and LC properties induced by the cholesteric functionality in polymers.

The polymers studied in this project could result in a new kind of polymeric materials with appealing properties. The main goal of this project was to synthetize, characterize and analyze the properties of the side-chain cholesterol based linear liquid crystal polyurethanes. The procedure followed in the process was to synthetize and characterize a new cholesterol derivative monomer to then homopolymerize and copolymerize it. As a result, different formulations of the desired polymeric liquid crystals were obtained, thermal and optical properties were analyzed in ulterior studies and their liquid crystalline behaviour. This kind of materials could suppose the opening of a path to new materials with optical and biotechnological applications research.

RESUMEN

Actualmente los cristales líquidos poliméricos son uno de los materiales poliméricos más estudiados para el desarrollo de nuevas tecnologías ópticas y fotónicas. Las exclusivas propiedades que presentan los LCPs iniciaron una nueva corriente de investigación en química polimérica que ha dado lugar a una gran variedad de dispositivos de uso tanto especializado como cotidiano. Por otro lado, el auge de polímeros basados en colesterol diseñados para aplicaciones biotecnológicas en liberación controlada de fármacos incentivó el estudio del punto de confluencia entre las propiedades biotecnológicas y de cristal líquido inducidas por la funcionalidad colestérica en polímeros.

Los polímeros estudiados en este proyecto podrían resultar en una nueva gama de materiales de interesantes propiedades. Por lo tanto, el objetivo principal de este proyecto ha sido la síntesis y caracterización de nuevos cristales líquidos poliméricos con ramificaciones de colesterol basados en poliuretanos lineales. El procedimiento seguido consistió en la síntesis y caracterización de un nuevo monómero derivado del colesterol para después ser homopolimerizado y copolimerizado. Como resultado, se obtuvieron a diferentes formulaciones de los cristales líquidos objetivo, de los cuales se analizaron posteriormente sus propiedades térmicas y ópticas confirmándose su comportamiento de cristal líquido. Este tipo de materiales podrían suponer la apertura de un nuevo camino a futuras investigaciones en materiales para aplicaciones en óptica y biotecnología.

INDEX:

1. GLOSSARY:

BDEC: Benzyl diethanolcarbamate (Benzyl bis(2-hydroxyethyl)carbamate).

BLP: Blank linear polyurethane.

CDEC: Cholesteryl diethanolcarbamate (Cholesteryl bis(2-hydroxyethyl)carbamate).

ChX-LCP: "Ch" refers to "Cholesterol" and X stands for its molar ratio in the LCP, ranging from 0 to 100.

DCM: Dichloromethane.

DEA: Diethanolamine.

DSC: Differential scanning calorimetry.

Đ: Polymers polydispersity index.

FTIR: Fourier-transform infrared spectroscopy.

HDI: Hexamethylene diisocyanate.

LC: Liquid crystal.

LCP: Liquid crystal polymer.

M_n: Number average molar mass.

NMR: Nuclear magnetic resonance.

M_w: Weight average molar mass.

POM-S: Polarized optical microscopy and spectroscopy.

PPG_{1000}: Polypropylene glycol of 1000Da average molar mass.

PU: Polyurethane.

Rf: Thin layer chromatography retention factor.

SEC-GPC: Size exclusion chromatography - Gel permeation chromatography.

SLP: Sample of linear polyurethane.

Td: Degradation temperature assigned to a 5% mass loss.

TGA: Thermogravimetric analysis.

THF: Tetrahydrofuran.

WAXS: Wide angle X-ray scattering.

2. INTRODUCTION:

From a classical point of view, materials can be sorted in three distinct groups depending on their degree of order: solid-crystalline, liquid and gases or plasma. The degree of order in the material is always related to the surrounding temperature and pressure. However, many non-classical condensed states of matter have been described over a century ago such as the amorphous glass and the liquid crystal phases. Liquid crystals (LCs) and liquid crystal polymers (LCPs) are additional condensed states of matter displayed by certain organic substances, i.e. some special class of polymers. The distinctive characteristic of liquid crystal phases, known as mesophases, is due to the combination of a structure with certain degree of order (positional and/or orientational) and the capacity to flow assuming the shape of the recipient. This capacity gives to the material unique properties that allowed the development of new technologies such as the well-known LC displays. Furthermore, there are currently many other fields where this kind of materials are present, such as gas and temperature detectors, optical information storage devices or piezoelectric generators.

LC behaviour relies on the phase constituent molecules or polymeric units known as mesogens. Molecular anisotropy, in either shape (rod-like, most commonly) and/or solubility (amphipathicity), is required to get a balanced interaction between molecules allowing their free movement favoring their capacity to adopt an ordered but fluid structure. The most common mesogenic units consist of rod-shaped structures which contain a side chain, multiple aromatic rings, and a terminal group on the opposite side. In contradistinction to common isotropic liquids, LC materials always display a high orientational order, but the positional ordering varies within a wide range from one structure to another. Nonetheless, the orientational order of mesogens in the LC phases is not perfect [Figure 1], which leads to light scattering effects while being observed under the microscope.[1]

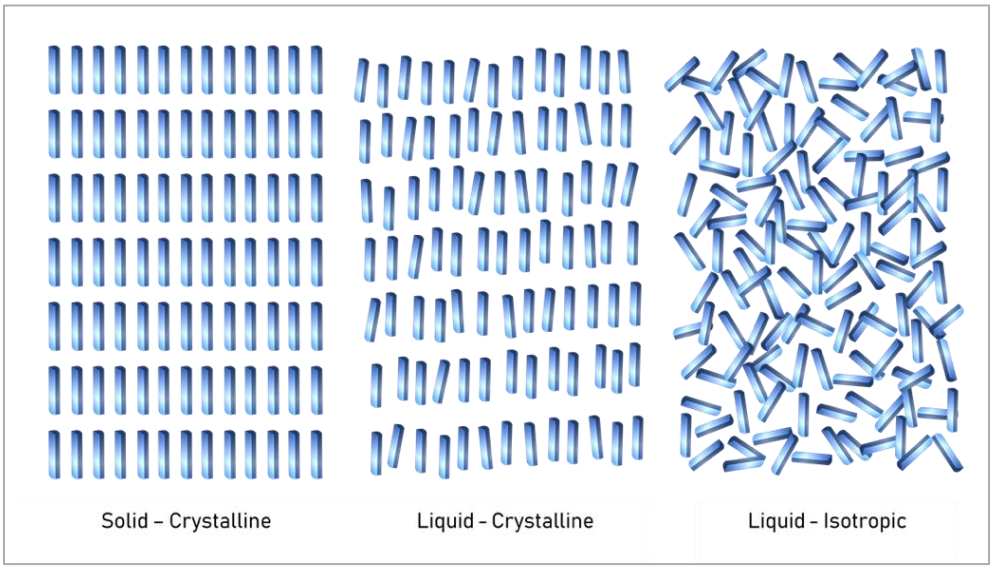

Figure 1. Schematic representation of different physical states of mesogenic molecule layers.

The differences between each mesophase class are due to the relative positional orientation of the LC molecules. Depending on the kind of LC, each mesophase is only stabilized in a specific pressure, temperature or concentration interval. Based on this definition, many materials can be categorized as liquid crystals with different classifications depending on their physical properties: lyotropic (concentration), electrotropic (potential difference) or thermotropic (temperature).

An explanation for the thermotropic liquid crystal behaviour consists on the mentioned anisotropic physical interaction between molecules, which is in constant competition with the same molecules' thermal motion. Therefore, the resultant equilibrium makes the liquid-crystal phase stable within a specific temperature interval. If a material with thermotropic properties that can present different kind of mesophases undergoes through a heating process, the mesophase transition course would start from the most ordered structured mesophase to a less ordered phases until reaching the isotropic state. Many different mesophases [Figure 2] have been discovered in the last decades: nematic, smectic, chiral, columnar, calamitic and blue phases among others. Despite the wide range of phase structures, the most commonly studied mesophases are the different nematic and smectic and their chiral variations because of their higher structural simplicity or unique physical properties.[2]

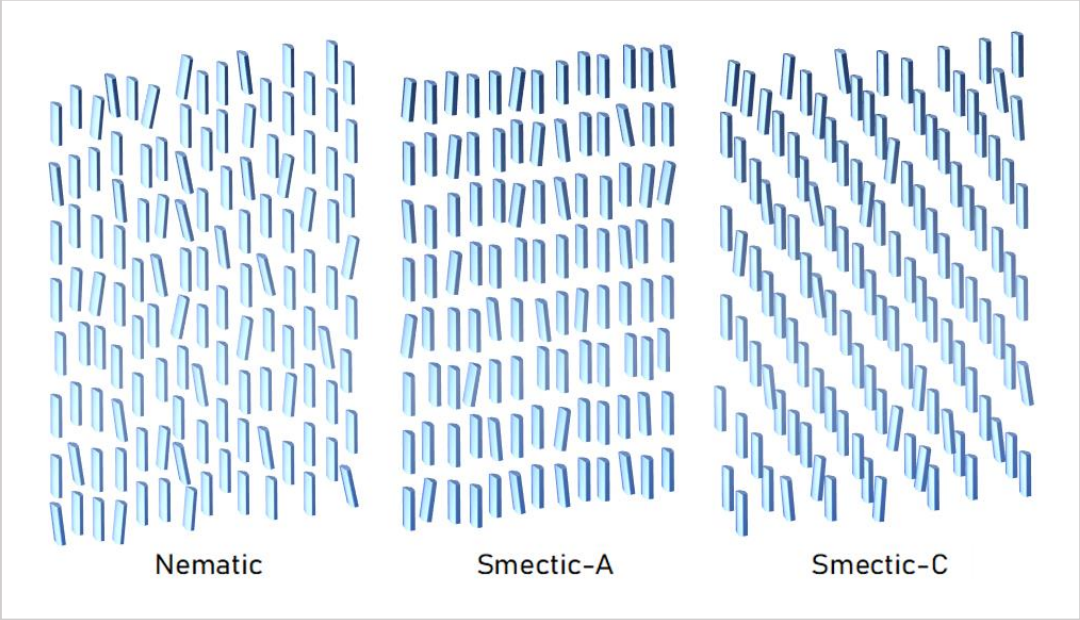

Figure 2. Schematic representation of Nematic, Smectic-A and Smectic-C liquid crystal phase layers where the blue tiles represent the mesogenic molecules of a LC material.

The growing interest in liquid crystal polymers was originated because they hold a combination of the properties conventional LCs and the widely used thermoplastic polymers. This combination leads to a kind of polymeric material with interesting thermal behaviours. Whereas molten conventional plastics display isotropic phases, liquid crystal polymers exhibit liquid crystalline properties in melt conditions. Although LCPs exhibit the same phases as conventional liquid crystalline compounds, their melting point are usually found at much higher temperatures (100-300°C). Additionally, as thermoplastic polymers, some LCPs display a glass transition temperature depending on their composition.

The key to induce a LC behaviour in a thermoplastic polymer is to provide movement and rotational restrictions to the polymer chains, which in this case is provided by the stiffness generated by the mesogenic units. The induced steric hindrance between mesogens rigidifies the chains restricting their rotation freedom and forcing them to be close to each other in specific structural arrangements. Furthermore, depending on how the mesogenic units are integrated into the polymeric chain, different kind of LCP morphologies can be considered [Figure 3].

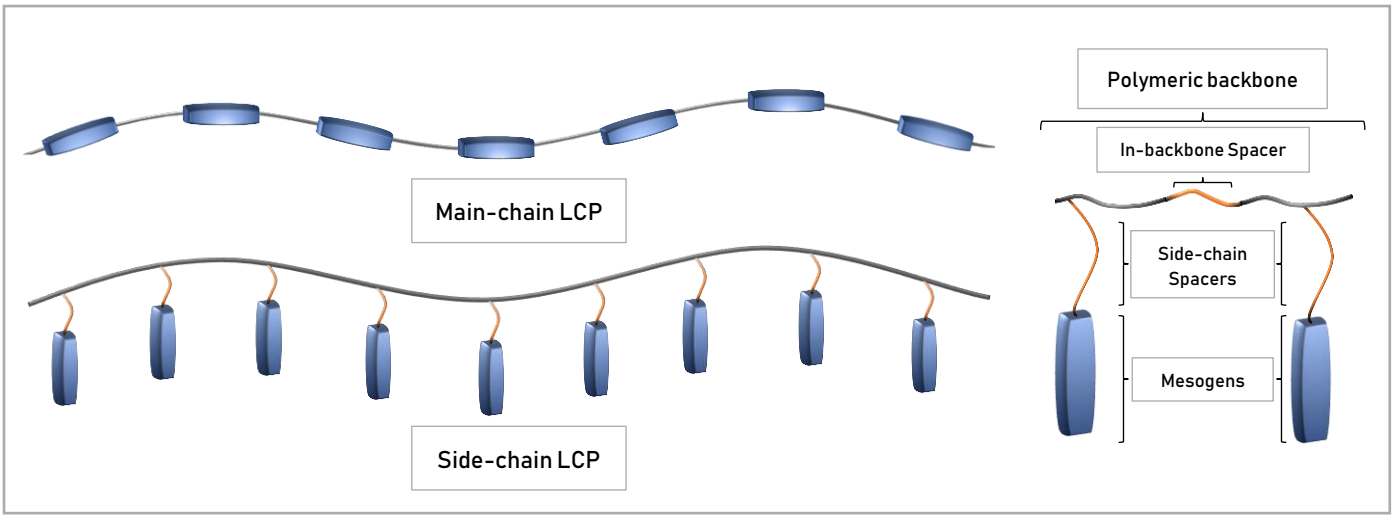

Figure 3. Main-chain and Side-chain LCP structure schemes.

Main-chain LCPs have mesogen units in their backbone that create stiff regions allowing the polymer chains to assemble in liquid crystalline structures. Conversely, side-chain LCPs have their mesogen units pending from their polymeric chain. The resulting structures can be divided in three different subunits: the polymer backbone, the mesogenic group and an optional flexible spacer. The spacers, can either link the mesogenic unit to the polymer backbone or separate the mesogenic residues in the actual backbone, affecting the material's mobility. Each individual component has an effect on the final properties of the obtained LCPs.[3]

Some of the most interesting polymers to incorporate this kind of LC structures are polyurethanes. Polyurethanes (PUs) constitute one of the most important type of polymeric materials with uses ranging from high performance structural applications to foam padding. Due to their diverse utility and relatively low cost, these materials account for nearly 5 wt % of total worldwide polymer production and are expected to exceed 18 kilotons annually by 2016. Based on the original discovery by Bayer, linear PUs are usually prepared by a step-growth polyaddition route [Figure 4] involving the reaction of diols with diisocyanates in the presence of a catalyst.[4,5]

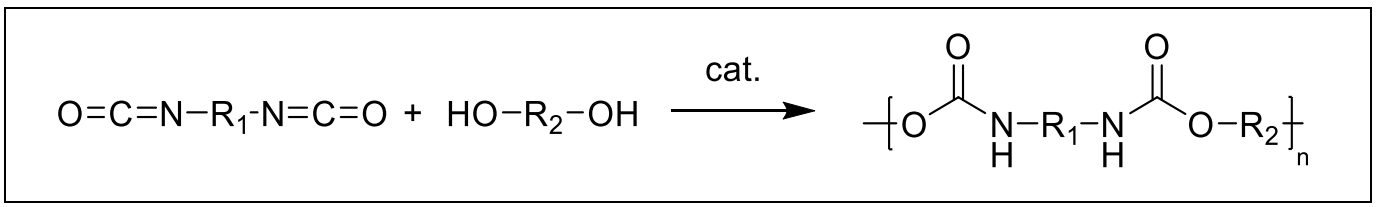

Figure 4. Polyurethane production path by a polyaddition reaction.

Based on all mentioned statements, the synthetized LCPs were chosen to be cholesterol based polyurethanes, where the cholesteric function was selected as side-chain mesogenic unit. The choice of the cholesteric functionality for this project LCP is due to the well-known optical properties displayed by cholesterol derivatives as well as the biological properties associated to its structure.[6]

The cholesterol structure contains a polar hydroxyl group and a non-polar bulky steroid with a hydrocarbon iso-octyl side chain 'tail' that gives to the molecule amphipathic properties; this makes the molecule anisotropically hydrophilic and lipophilic. The combination of the rigidity of the steroid structure and the flexibility of the hydrocarbon tail gives to the cholesterol molecule the ability of orientational ordering, which is required to display a liquid crystalline behaviour in combination with lipid membrane binding properties.[7]

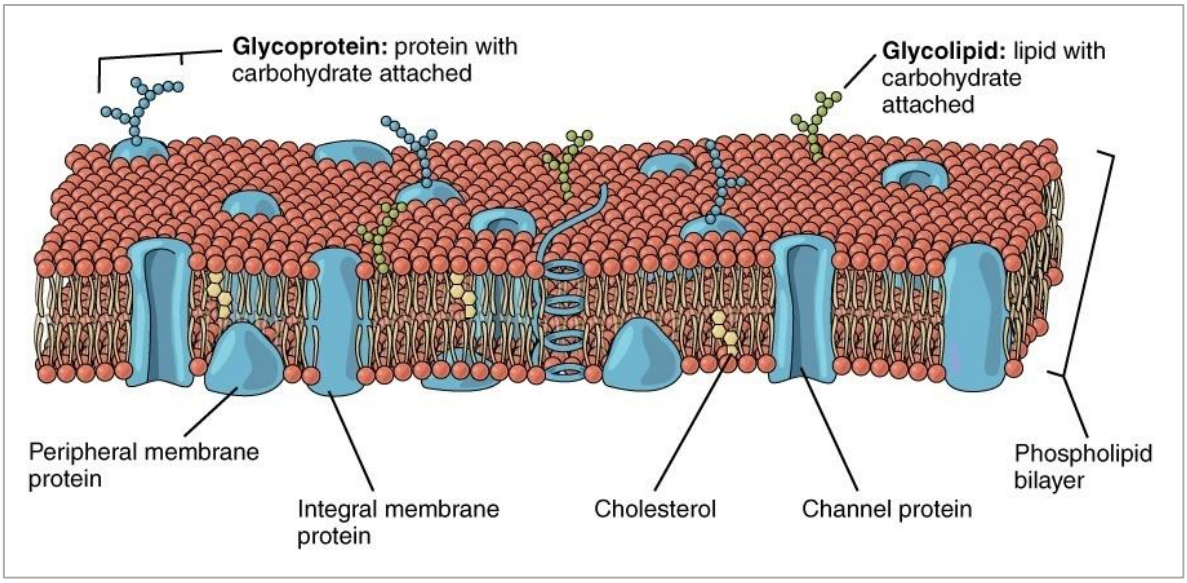

Figure 5. Animal cell lepidic bilayer scheme were the cholesterol molecules can be seen anchored to the structure.[8]

The presence of the cholesterol functionality in liposomes has been proven to enhance the stabilization of drug delivery in addition to serve as an anchoring unit for liposome fixation mechanisms. Also, the cholesterol presence is required to all animal cell membranes [Figure 5] and liposomes, to maintain their integrity, and modulate the fluidity and permeability without mobility loss consequences. As result of this functions, cholesterol affects to several cellular processes and makes it a great valuable resource for many biotechnological and analytical applications. Cholesterol's hydroxyl group or its polar derivative interact with the polar heads of the membrane phospholipids and sphingolipids, while the tailed-steroid hydrocarbon structure permeates into the nonpolar inner membrane region affecting its molecular sorting, trafficking and cell signaling properties. This binding faculty provides the synthetized cholesterol based polymeric surfaces with properties for cell-membrane interaction and liposome anchoring. Thus, combining cholesterol based polymers with drug delivery liposomes, regulates the tendency to leak the entrapped molecules through the lipid bilayer and increases the circulation time through the bloodstream as they act as stabilizing anchoring units. [9]

Moreover, recent studies have proven a correlation between physical properties of cellular plasma membranes and its cholesterol content, affecting to the residing receptors and enzymes activity. Among other roles, cholesterol acts as a synthesis precursor of bile acids and assists the metabolization processes of fat soluble vitamins such as A, D, E and K. Therefore, the interaction between the synthetized polymers and cells could affect to their inner behaviour functions and metabolic behaviour. Furthermore, the high cholesterol content stiff regions could act as cell grow favored areas while the polypropylene glycol residues could act as borders, delimiting the mentioned cell growth.

3. PROJECT OBJECTIVES:

This project objectives were divided in two different parts. The aim of the first part of this project was to synthetize a new class of polymeric liquid crystals based on linear polyurethanes with cholesteric functionalities as side-chain units. The incorporation of cholesterol is thought to induce liquid crystal behaviour in addition to interesting biotechnological properties. In order to obtain the desired side-chain linear polymers, an adequate cholesterol derivative monomer was synthetized and then polymerized with hexamethylene diisocyanate (HDI) using an organotin compound as a catalyst. Beside the cholesteric units, additional copolymers were synthetized incorporating different ratios of polypropylene glycol (PPG) to the polymer formulation as an in-backbone spacer unit [Figure 6]. The copolymerization resulting materials presented soft regions that broadened the temperature ranges where polymeric chains allowed a liquid crystal behaviour regardless of the stiffness created by the cholesteric residues.

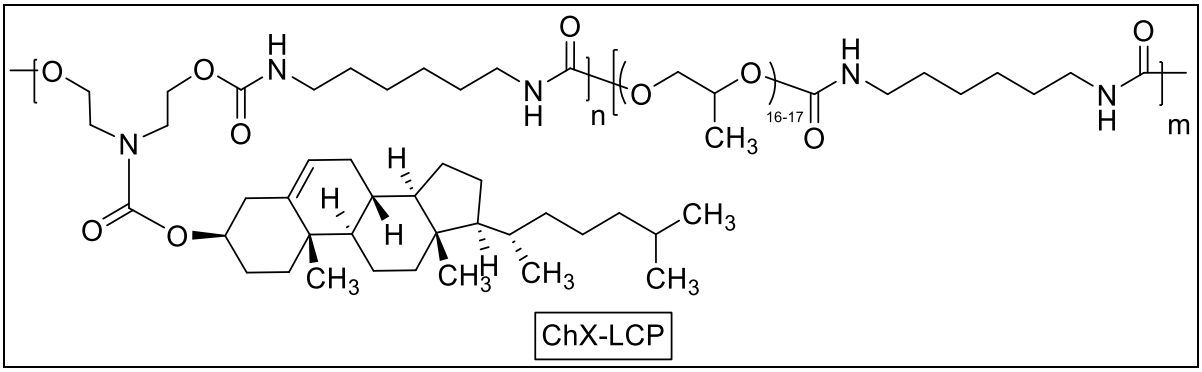

Figure 6. Structure of the synthetized copolymers, where the side-chain cholesteric group as mesogenic unit and the PPG residue as in-backbone spacer unit can be observed.

In the second part, the two goals were the characterization of the obtained polymers through different techniques and the analysis of its liquid crystal properties. For the characterization, conventional techniques such as nuclear magnetic resonance (NMR) or Fourier transform infrared spectroscopy (FT-IR) were used to confirm that the formed species matched successfully the desired structures. To conclude, the target was the study of the liquid crystal properties using more specific techniques, including differential scanning calorimetry (DSC), polarized light microscopy (POM) and wide angle X-ray scattering (WAXS).

4. EXPERIMENTAL SECTION:

4.1. STARTING MATERIALS AND SOLVENTS:

Diethanolamine of Laboratory reagent grade (CAS: 111-42-2) was purchased from Fisher Scientific and used as supplied. Cholesteryl chloroformate purity 95% (CAS: 7144-08-3), hexamethylene diisocyanate purity ≥99.0% (CAS: 822-06-0), polypropylene glycol M_w average 1000g/mol (CAS: 25322-69-4), dibutyltin dilaurate Purity 95% (CAS: 77-58-7) and Chloroform-d 99.8 atom % D (CAS: 865-49-6) were purchased from Sigma Aldrich and used as supplied except for polypropylene glycol which had to be dried by azeotropic distillation with toluene. Benzyl chloroformate Purity 97% (CAS: 501-53-1) was purchased from Acros Organics and used as supplied. For the solvents: tetrahydrofuran, methanol and toluene were purchased form Fisher Scientific and n-hexane fraction from petroleum, ethyl acetate, dichloromethane, chloroform and methanol were purchased from Scharlab, S.L. all solvents were used as supplied.

4.2. CHARACTERIZATIONS METHODS:

^{1}H and ^{13}C Nuclear Magnetic Resonance (NMR) spectra were recorded at room temperature with Bruker Avance DPX 300 spectrometer at 300.16MHz and 75.5MHz of resonance frequency ^{1}H and ^{13}C spectra respectively, using deuterated and chloroform as solvent. The experimental conditions for the ^{1}H NMR were near to 10mg of sample, 3s acquisition time, 1s delay time, 8.5µs pulse, spectral width 5000 Hz and 32 scans. For the ^{13}C NMR 40mg of sample, inverse gated decoupled sequence, 3s acquisition time, 4s delay time, 5.5µs pulse, spectral width 18,800Hz and more than 10,000 scans. The NMR chemical shifts were reported as δ in parts per million (ppm) relative to the traces of non-deuterated solvent (δ = 7.26 for $CDCl_3$). Data were reported as: chemical shift, multiplicity (s = singlet, d = doublet, t = triplet, m = multiplet, br = broad), coupling constants (J) given in Hertz (Hz), and integration. Standard ^{1}H was used to characterize every monomer and reactant used. Quantitative ^{1}H NMR spectra were carried out to confirm the ratio of different monomers in the polymer and ^{13}C NMR was used to characterize the polymer structure.

Fourier-transform infrared spectroscopy (FTIR) spectra were obtained by FTIR spectrophotometer (Nicolet 6700 FT-IR, Thermo Scientific Inc., USA) using transmission FTIR technique with the samples casted over KBr pellets from a solution with THF as solvent. Spectra were recorded between 4000-525 cm^{-1} with a spectrum resolution of 4 cm^{-1}. All spectra were averaged over 10 scans. This technique was used to follow the polymer reaction kinetics by analyzing the characteristic signal of the isocyanate group which decreases due to its conversion. Data were reported as: wavelength (cm^{-1}), for defined shapes (br = broad, sh = sharp) and intensity (s = strong, m = medium, w = weak).

Size exclusion chromatography – Gel permeation chromatography (SEC – GPC). SEC was performed in at 30° C as eluent using a Waters chromatograph equipped with four 5 mm Waters columns (300 mm “x” 7.7 mm) connected in series with increasing pore sizes. Tetrahydrofuran was used as eluent and Toluene was used as a marker. Polystyrenes of different molecular weights ranging from 2,100 g mol^{-1} to 1,920,000 g mol^{-1}, and low polydispersity indexes were used for the calibration.

Thermogravimetric analysis. A thermogravimetric analyzer (TGA-Q500 V20, TA Instrument Inc., USA) was used to study the thermal stability limits of the samples. A total of 5-10 mg of samples was heated from 25°C to 800°C at a heating rate of 10°C/min under N_2 atmosphere (50mL/min).

Differential Scanning Calorimetry. A differential scanning calorimeter (DSC-Q2000, TA Instrument Inc., USA) was used to analyze the thermal behaviour of the samples under N_2 atmosphere to determine the glass transition temperatures and liquid crystal phase transition temperatures. A total of 6-8 mg of previously dried samples were placed in sealed aluminum pans and heated using a heating rate from -70°C to 200 or 215°C at a heating rate of 10°C/min to remove the thermal history of the samples. The samples were then cooled to -70°C and reheated to 200 or 215°C at 10°C/min. The glass transition and melting temperatures were obtained from the second heating run.

Polarized optical microscopy and spectroscopy (POM-S). Among many applications that rely on plane-polarized light, the polarized optical microscopy (POM) can be described as a fundamental technique for the study of LC materials. For the measurements, samples were positioned in the hot stage between the polarizer and the analyzer (Linkam Scientific Instruments Ltd.) in a Zeiss Axio Scope A1 microscope with 10X objective lens. The analyzer was positioned with its permitted vibration directions at ninety degrees respect the first polarizer. Thus, only the extraordinary light waves generated due to the samples' birefringence pass through the analyzer. Therefore, a non-birefringent sample placed in the hot stage would negate the light pass through the system displaying a dark field view in the eyepieces. Consequently, isotropic and anisotropic materials can be distinguished by POM. The required light intensity was provided by a bright-field tungsten-halogen bulb and the obtained spectra were recorded by the spectrometer (Ocean Optics USB2000+) and the images captured by the installed camera (Zeiss Axiocam 105 Color) which were positioned at the end of the light path, just after the analyzer. To determine the phase transition temperatures, the samples were heated at a constant rate while images and spectra (in visible wavelength region) were simultaneously collected. Under a N_2 atmosphere, a heating rate of 10°C/min was applied and the mean values of three consecutive spectra every 5°C and 30s were acquired. To study the samples birefringence, the transmitted intensity at each temperature spectra was then integrated between the suitable wavelength range (480 to 700 nm) to obtain the value of the total intensity transmitted through the materials.

X-Ray Scattering. In this study, we LC structure formation processes during heating and cooling rates were studied with measurements of wide-angle X-ray scattering (WAXS) using synchrotron radiation. These experiments were performed at BL11 NCD-SWEET beamline at ALBA Synchrotron with the collaboration of ALBA staff. The developed measurement involved the following steps: the sample powder is introduced in borosilicate capillary (1.5mm) and placed in a Linkam hot stage place in the incident X-ray beam. The sample was first heated up to isotropic melt at a rate of 20 °C/min^{-1} recording a pattern every degree. After that, the melt was cooled down at a cooling rate of 20 °C/min^{-1} and heated up again under the same conditions. The exposure time of each shot and the time interval between the measurements were 2.5 and 0.5s.

4.3. MONOMER AND LINEAR POLYURETHANE SYNTHESIS:

4.3.1. SYNTHESIS OF CHOLESTERYL DIETHANOLCARBAMATE (CDEC):

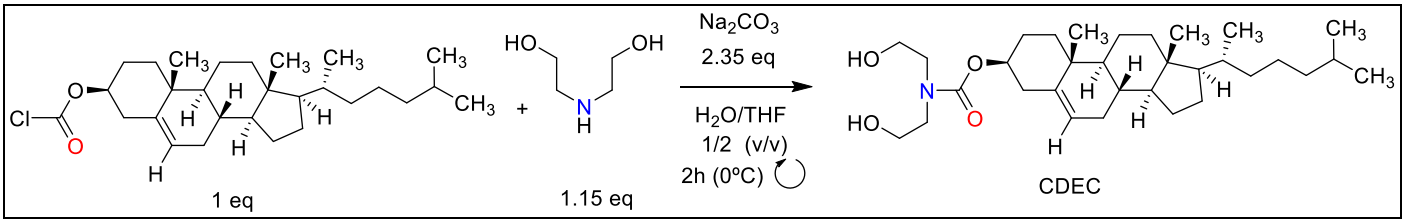

Figure 7. Simplified CDEC synthesis reaction.

In a round bottom flask (250 mL) equipped with a magnetic stir bar, diethanolamine (1.17g, 11.10 mmol, 1.15 eq.) and Na_2CO_3 (2.41g, 43.07mmol, 2.35 eq.) were added in a mixture of DI water (15 mL) and tetrahydrofuran (THF 30 mL). The reaction mixture was cooled in an ice-bath for about 20 min. To the mixture cholesteryl chloroformate (4.34g, 9.66 mmol, 1 eq.) was added in one portion and the reaction was allowed to proceed in ice-cold conditions for 2h, followed by 2h at room temperature. Ethyl acetate (EA, 50 mL) was added to the reaction mixture and the organic layer was isolated and to the remaining aqueous layer, saturated NH_4Cl aqueous solution (40 mL) was added. The aqueous layer was twice extracted with EA (50 mL) and the organic layers were combined and dried over $MgSO_4$ and the volatiles were removed under vacuum. As a result, 4.96g of the product were obtained [Figure 7], $CHCl_3$/EtOAc (9:1 v/v) Rf = 0.68.

CDEC: White solid; yield 99%. **^{1}H-NMR** (300.16 MHz, $CDCl_3$): δ = 0.68 (s, 3H, CH_3), 0.85-0.87 (d, 3H, J = 0.2 Hz, CH-C$\underline{H}_3$), 0.86-0.88 (d, 3H, J = 0.2 Hz, CH-C$\underline{H}_3$), 0.90-0.92 (d, 3H, J = 0.2 Hz, CH-C$\underline{H}_3$), 1.01 (s, 3H, J = 0.2 Hz, C-C$\underline{H}_3$), 0.94-2.45 (m, 29H, Cholesteric aliphatic C$\underline{H}$, C$\underline{H}_2$), 3.49 (br, 4H, O-CH$_2$-C$\underline{H}_2$-N), 3.83 (br, 4H, O-C$\underline{H}_2$-CH$_2$-N), 4.54 (m, 1H, ***), 5.38 (d, 1H, C=C$\underline{H}$-CH$_2$). **^{13}C-NMR** (75.5 MHz, $CDCl_3$): δ = 12.00 (s, 1C, CH_3), 18.85 (s, 1C, CH_3), 19.52 (s, 1C, CH_3), 21.18 (s, Ch-2°/3°/4° Ch-2°,3°,4°-C), 22.70 (s, 1C, CH_3),22.95 (s, 1C, CH_3), 24.00-48.39 (s, Ch-2°,3°,4°-C), 50.13 (s, 2C, $\underline{C}H_2$-NH-C=O), 56.28- 56.80 (s, Ch-2°,3°,4°-C), 61.99 (s, 2C, $\underline{C}H_2$-OH), 75.45 (s, 1C, CH-O-C=O), 122.78 (s, 1C, C=$\underline{C}$H), 139.77 (s, 1C, $\underline{C}$=CH), 156.87 (s, 1C, C=O). **FT-IR** (KBr): $\tilde{\nu}$ (cm^{-1}) = 3415 (m-br, υ = O-H), 3020 (w, υ= C_{sp2}-H) ,2963 (s, υ= C_{sp3}-H) ,2938 (s, υ= C_{sp3}-H) ,2888-2866 (s-br, υ= C_{sp3}-H) ,1680 (s, υ= C=O $_{\text{Amide I}}$) ,1630 (m, υ= C=C) ,1470 (s-sh, δ= CH_3 + CH_2 $_{\text{Scissoring}}$) ,1376+1367 (m, δ= CH_3 $_{\text{Umbrella}}$) ,1264 (m, υ= C-N $_{\text{Amide III}}$) ,1230 (m, υ= C-O) ,815 (w, $\delta_{(o.o.p.)}$= C=C-H) ,618 (w-br, $\delta_{(o.o.p.)}$= N-H).

4.3.2. SYNTHESIS OF BENZYL DIETHANOLCARBAMATE (BDEC):

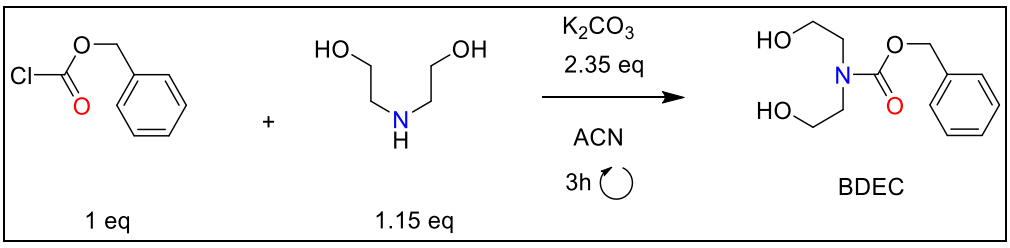

Figure 8. Simplified BDEC synthesis reaction.

In a round bottom flask (50mL) equipped with a magnetic stir bar, to a solution of diethanolamine (1.76g, 16.72 mmol, 1 eq.) in acetonitrile (20 mL) K_2CO_3 (5.25 g, 38.04 mmol) and benzyl chloroformate (2.85g, 16.72 mmol, 1 eq.) were added. The suspension was stirred vigorously for 3h at 0°C. After, a saturated NaCl solution (50mL) and DCM (30mL)

were added and the organic phase was isolated. To the remaining aqueous phase was rinsed three times with DCM (15mL) and the organic layer was dried, filtered and concentrated to afford Intermediate. The organic layers were combined and dried over $MgSO_4$ and the volatiles were removed under vacuum. As a result, 3.81g of product were obtained [Figure 8], DCM/MeOH (9:1 v/v) Rf = 0.71.

BDEC: Pink oil; yield 95%. **^{1}H-NMR** (300.16 MHz, $CDCl_3$): δ = 3.41 (s, 2H, HO-CH_2-CH_2-N), 3.49 (br, 4H, HO-CH_2-CH_2-N), 3.71-3.87 (br, 4H, HO-CH_2-CH_2-N), 5.13 (s, 2H, CH_2-Ph), 7.28-7.39 (m, 5H, Ph-H).

4.3.3. SOLUTION STEP-GROWTH SYNTHESIS OF LINEAR POLYURETHANES:

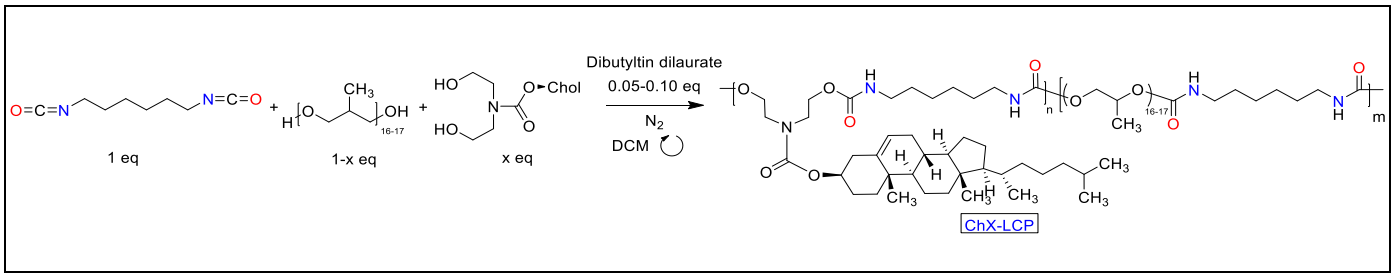

Figure 9. Simplified synthesis reaction for the ChX-LCPs synthesis.

To synthetize each individual polyurethane [Table 1], the required quantities of the previously dried diols (PPG, CDEA, BDEA) were solubilized in THF (5mL) and stirred at RT for 5 minutes. To the diol mixture the required HDI quantity was added followed by the catalyst (DBTDL). The reactions were left under N_2 atmosphere at RT and under vigorous stirring for 4-6 days [Figure 9].

Table 1. Molar quantities required for each polymer synthesis.

Polymer label	Reaction component (mmol)				
	HDI	PPG	CDEC	BDEC	DBTDL
SLP	1.7120	1.7120	-	-	0.0893
BLP	4.9083	-	-	4.9083	0.2454
Ch10-LCP	1.7857	1.6072	0.1786	-	0.0933
Ch20-LCP	1.8661	1.4929	0.3732	-	0.1079
Ch50-LCP	2.1573	1.0786	1.0786	-	0.2556
Ch80-LCP	2.5561	0.5112	2.0449	-	0.2724
Ch90-LCP	2.7240	0.2724	2.4516	-	0.2916
Ch100-LCP	2.9155	-	2.9155	-	0.0856

Once each reaction kinetics showed a total conversion, the PUs were purified. Each polymer solution obtained was divided on two fractions and transferred to Falcon tubes (50mL). To the solutions a precipitant was added dropwise filling 40mL of the tubes (n-hexane for every PU except for the LCP with more than 0.5 eq. of CDEA for which methanol was used), to increase the amount of precipitated polymer the mixtures were chilled by immersing the tubes

in liquid N_2 for 30 - 60s. To separate the polymers from the liquid phase the samples were centrifuged at 15.000rpm for 5min. In order to eliminate the remaining volatiles from the polymers, the samples were treated in a Vacuo-Temp desiccator at 90°C for 1h.

Ch100-LCP: White solid – **^{1}H-NMR** (300.16 MHz, $CDCl_3$): δ = 0.68 (s, 3H, CH_3), 0.85-0.87 (d, 3H, J = 0.2 Hz, CH-CH_3), 0.86-0.88 (d, 3H, J = 0.2 Hz, CH-CH_3), 0.90-0.92 (d, 3H, J = 0.2 Hz, CH-CH_3), 0.94-2.45 (m, 29H, Cholesteric aliphatic CH, CH_2), 1.01 (s, 3H, J = 0.2 Hz, C-CH_3), 1.33 (m, 2H, CH_2-CH_2-CH_2-NH-C=O), 1.49 (m, 2H, CH_2-CH_2-CH_2-NH-C=O), 3.10-3.18 (d, 2H, J = 0.02 CH_2-CH_2-CH_2-NH-C=O), 3.49 (br, 2H, N-CH_2-CH_2-O-C=O), 4.17 (br, 2H, N-CH_2-CH_2-O-C=O), 4.50 (m, 1H, CH-O-C=O), 5.35-5.36 (d, 1H, J = 0.01 C=CH-CH_2). **^{13}C-NMR** (75.5 MHz, $CDCl_3$): δ = 12.00 (s, 1C, CH_3), 18.85 (s, 1C, CH_3), 19.52 (s, 1C, CH_3), 21.18 (s, Ch-2°,3°,4°-C), 22.70 (s, 1C, CH_3), 22.95 (s, 1C, CH_3), 23.99-24.42 (s, Ch-2°,3°,4°-C), 26.43 (s, CH_2-CH_2-CH_2-NH-C=O), 28.14-28.36 (s, Ch-2°,3°,4°-C), 29.91 (s, CH_2-CH_2-CH_2-NH-C=O), 32.00-39.86 (s, Ch-2°,3°,4°-C 40.96 (s, O=C-N-CH_2), 42.44 (s, Ch-2°,3°,4°-C), 50.13 (s, 1C, CH_2-NH-C=O), 52.16-56.80 (s, Ch-2°,3°,4°-C),61.99, 75.45 (s, CH-O-C=O), 122.78 (s, 1C, C=CH), 139.77 (s, 1C, C=CH),155.81 (s, 1C, Ch-O-C=O), 156.87 (s, 1C, O=C-CH_2-CH_2-N). **FT-IR** (KBr): $\tilde{\nu}$ (cm^{-1}) = 3407 (m, υ = N-H), 3338 (m-br, υ = H-O $_{Humidity}$), 2933 (s, υ= C_{sp3}-H), 2866 (m, υ = C_{sp3}-H), 2850 (m, υ = C_{sp3}-H), 1700 (s, υ = C=O $_{Amide\ I}$), 1540 (m, δ = N-H $_{Amide\ II}$), 1465 (m, δ = CH_3 + δ = CH_2 $_{Scissoring}$), 1379 + 1364 (m, δ = CH_3 $_{Umbrella}$), 1270 - 1243 (br, υ = C-N $_{Amide\ III}$ + υ = C-O), 618 (w-br, $\delta_{(o.o.p.)}$ = N-H).

SLP: Translucent solid. **^{1}H-NMR** (300.16 MHz, $CDCl_3$): δ = 1.12-1.15 (m, 3H, CH_3-CH-O-CH_2), 1.21 (br, 3H, CH_3-CH-CH_2-O-C=O), 1.23 (br, 3H, CH_3-CH-O-C=O), 1.32 (br, 4H, CH_2-CH_2-CH_2-NH-C=O), 1.48 (br, 4H, CH_2-CH_2-CH_2-NH-C=O), 3.08-3.20 (m, 4H, CH_2-NH-C=O), 3.33-3.46 (m, 1H, $H^{pro\text{-}R}$-CH-O-CH), 3.47-3.60 (m, 2H, $H^{pro\text{-}S}$-CH-O-[CH/H] + CH_3-CH-O-[CH_2/H]), 4.75 (br,1H, $H^{pro\text{-}R}$-CH-O-C=O), 4.90 (m, 2H, $H^{pro\text{-}S}$-CH-O-CH + CH_3-CH-O-C=O). **^{13}C-NMR** (75.5 MHz, $CDCl_3$): δ = 17.00-17.46 (m, CH_3-CH-O), 26.03-26.40 (m, CH_2-CH_2-CH_2-NH-C=O),29.30-30.30 (m, CH_2-CH_2-CH_2-NH-C=O),40.03 (s, CH_2-CH_2-CH_2-NH-(C=O)-CH_2), 40.70 (s, CH_2-CH_2-CH_2-NH-(C=O)-CH), 69.95 (s, CH-CH_2-OH), 71.84 (s, CH-CH_2-OH), 72.87 (s, CH_2-CH-O-H + CH-CH_2-O-H), 73.30 (s, CH-CH_2-O-H), 75.07-75.54 (m, CH-O-CH_2), 156.19 (s, O=C-NH-CH_2), 156.38 (s, O=C-NH-CH). **FT-IR** (KBr): $\tilde{\nu}$ (cm^{-1}) = 3333 (m-br, υ = N-H + υ = H-O $_{Humidity}$), 2970 (s-sh, υ = C_{sp3}-H), 2930 (s, υ = C_{sp3}-H), 2905-2780 (m-br, υ = C_{sp3}-H), 2265 (w-br, υ = O=C=N $_{Residual}$), 1720 (s, υ = C=O $_{Amide\ I}$), 1543 (m, δ = N-H $_{Amide\ II}$), 1462 (m, δ = CH_3 + δ = CH_2 $_{Scissoring}$), 1370 (m, δ = CH_3 $_{Umbrella}$), 1272 + 1254 (m, υ= C-N $_{Amide\ III}$ + υ = C-O $_{Urethane}$), 1110 (s-br, υ = C-O-C $_{polyol}$), 631 (w-br, $\delta_{(o.o.p.)}$ = N-H).

BLP: White solid. **^{1}H-NMR** (300.16 MHz, $CDCl_3$): δ = 1.25 (br, 4H, CH_2-CH_2-CH_2-N-C=O), 1.45 (br, 4H, CH_2-CH_2-CH_2-N-C=O), 3.01-3.18 (br, 4H, CH_2-NH-C=O), 3.44-3.62 (br, 4H, O=C-N-CH_2-CH_2-O-C=O), 4.09-4.28 (br, 4H, O=C-N-CH_2-CH_2-O-C=O), 5.12 (s, 2H, Ph-CH_2-O-C=O), 7.28-7.38 (m, 5H, Ph-H).

Copolymers – Ch90/80/50/20/10-LCP: White solid – **^{1}H-NMR** (300.16 MHz, $CDCl_3$): δ = 0.67 (s, 3H, CH_3), 0.85-0.87 (d, 3H, J = 0.2 Hz, CH-CH_3), 0.86-0.88 (d, 3H, J = 0.2 Hz, CH-CH_3), 0.90-0.92 (d, 3H, J = 0.2 Hz, CH-CH_3), 0.94-2.45 (m, 29H, Cholesteric aliphatic CH, CH_2), 1.01 (s, 3H, J = 0.2 Hz, C-CH_3), 1.21 (br, 3H, CH_3-CH-CH_2-O-C=O), 1.23 (br, 3H, CH_3-CH-O-C=O), 1.32 (br, 4H, CH_2-CH_2-CH_2-NH-C=O), 1.33 (m, 2H, CH_2-CH_2-CH_2-NH-C=O), 1.49 (br, 6H, CH_2-CH_2-CH_2-NH-C=O + CH_2-CH_2-CH_2-NH-C=O), 3.08-3.20 (q, 4H, J = 0.02 CH_2-CH_2-CH_2-NH-C=O + CH_2-NH-C=O), 3.33-3.60 (br, 5H, N-CH_2-CH_2-O-C=O + CH_2-O-[CH/H] + CH_3-CH-O-[CH_2/H]), 4.17 (br, 2H, N-CH_2-CH_2-O-C=O), 4.50 (m, 1H, CH-O-C=O), 4.90 (m, 2H, $H^{pro\text{-}S}$-CH-O-CH + CH_3-CH-O-C=O), 5.33-5.40z (br, 1H, C=CH-CH2). **^{13}C-NMR** (75.5 MHz, $CDCl_3$): δ = 12.00 (s, 1C, CH_3), 17.00-17.46 (m, CH_3-CH-O), 18.85 (s, 1C, CH_3), 20.90 (s, 1C, CH_3), 21.18 (s, Ch-2°,3°,4°-C), 22.40 (s, 1C, CH_3), 22.75 (s, 1C, CH_3), 23.79-24.22 (s, Ch-2°,3°,4°-C), 25.76-26.43 (m, CH_2-CH_2-CH_2-NH-C=O + CH_2-CH_2-CH_2-NH-C=O), 27.90-28.16 (s, Ch-2°,3°,4°-C), 29.30-30.30 (s, CH_2-CH_2-CH_2-NH-C=O + CH_2-CH_2-CH_2-NH-C=O), 31.78-39.68 (s, Ch-2°,3°,4°-C), 40.03-40.80 (s, O=C-N-CH_2 + CH_2-CH_2-CH_2-NH-(C=O)-CH_2 + CH_2-CH_2-CH_2-NH-(C=O)-CH), 42.24 (s, Ch-2°,3°,4°-C), 50.00 (s, 1C, CH_2-NH-C=O), 56.09-56.60 (s, Ch-2°,3°,4°-C), 72.87 (s, CH_2-CH-O-H + CH-CH_2-O-H), 73.30 (s, CH-CH_2-O-H), 75.55 (s, CH-O-C=O + CH-O-CH_2), 122.78 (s, 1C, C=CH), 139.77 (s, 1C, C=CH), 155.60 (s, 1C, O=C-O-Ch), 156.19 (s, O=C-NH-CH_2), 156.87 (s, 1C, O=C-CH_2-CH_2-N + O=C-NH-CH). **FT-IR** (KBr): $\tilde{\nu}$ (cm^{-1}) = 3338 (m-br, υ = N-H + υ= H-O $_{Humidity}$), 2933 (s, υ= C_{sp3}-H), 2866 (m, υ= C_{sp3}-H), 2850 (m, υ= C_{sp3}-H), 1700 (s, υ= C=O $_{Amide\ I}$), 1540 (δ= N-H $_{Amide\ II}$), 1465 (δ = CH_3 + δ = CH_2 $_{Scissoring}$), 1379 + 1364 (δ = CH_3 $_{Umbrella}$), 1270 - 1243 (υ = C-N $_{Amide\ III}$ + υ= C-O $_{Urethane}$), 1111 (υ = C-O-C $_{Polyol}$), 618 ($\delta_{(o.o.p.)}$ = N-H).

5. RESULTS AND DISCUSSION:

5.1. MONOMER SYNTHESIS AND CHARACTERIZATION:

5.1.1. MONOMER SYNTHESIS BY CHLOROFORMATE CARBAMATION REACTION:

The majority of conjugation strategies used to incorporate cholesterol units onto molecules of interest rely on esterification, carbamate, and carbonate bond formation using chloroformate derivatives. Since the desired monomer had to react with diisocyanates to give a linear polyurethane backbone, it was necessary to select a monomer with two aliphatic alcohols attached to it in addition to the cholesteryl functionality. To fulfill these requirements, the followed strategy consisted in the conjugation between two commercially available compounds: cholesteryl chloroformate and diethanolamine (DEA).

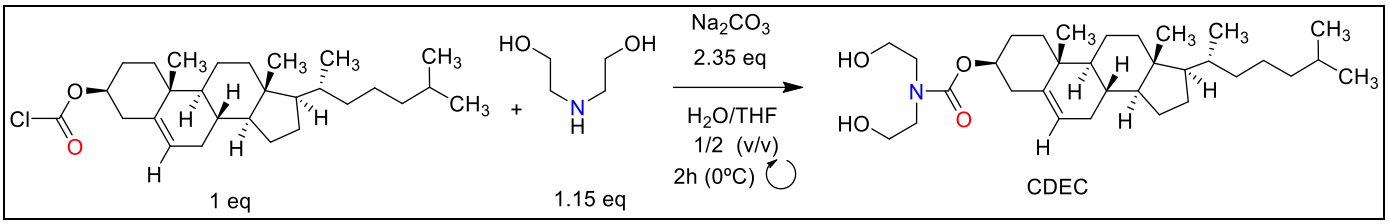

Figure 10. Simplified CDEC synthesis reaction.

The reaction [Figure 10] was carried out in a solution reaction media composed of Tetrahydrofuran (THF) and water at 0°C. THF was chosen as the organic primary component due to its capability to dissolve the hydrophobic cholesteryl chloroformate as well as the water soluble DEA. Although the common risk of working with chloroformates is the carbonation due to a reaction with water, in this case the cholesteryl functionality made the reactive highly hydrophobic. The obtained high yield for this reaction (99%) made only necessary a liquid-liquid extraction as required workup to isolate the pure product.

Additionally, to certify the registered thermal behaviour for the Ch-LCP polyurethanes is exclusively due to the cholesteryl functionality and not to the polymeric backbone, a similar monomer to CDEC was designed but with the cholesteryl functionality swapped for a benzylic group to be used as a blank [Figure 11]. The resulting benzyl bis(2-hydroxyethyl)carbamate (BDEC) was synthetized following a similar synthesis used for CDEC.

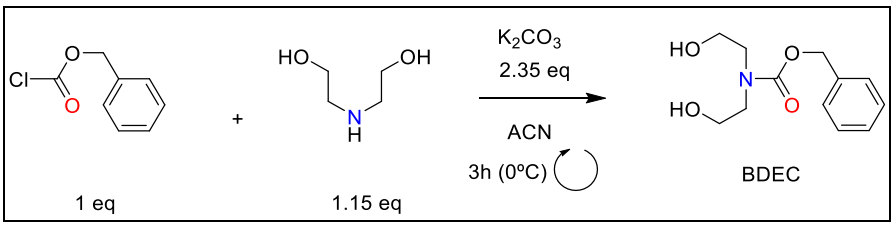

Figure 11. Simplified BDEC synthesis reaction.

5.1.1. MONOMER CHARACTERIZATION:

During this project, the CDEC monomer was synthetized with no available characterization data. Therefore an ^{1}H-NMR was performed [Figure***] to the synthesis product to ensure that the obtained compound matched the desired chemical structure without any visible side reaction compound traces. The molecule's protons were successfully assigned, allowing to proceed to the polyurethanes' synthesis [Figure 12].

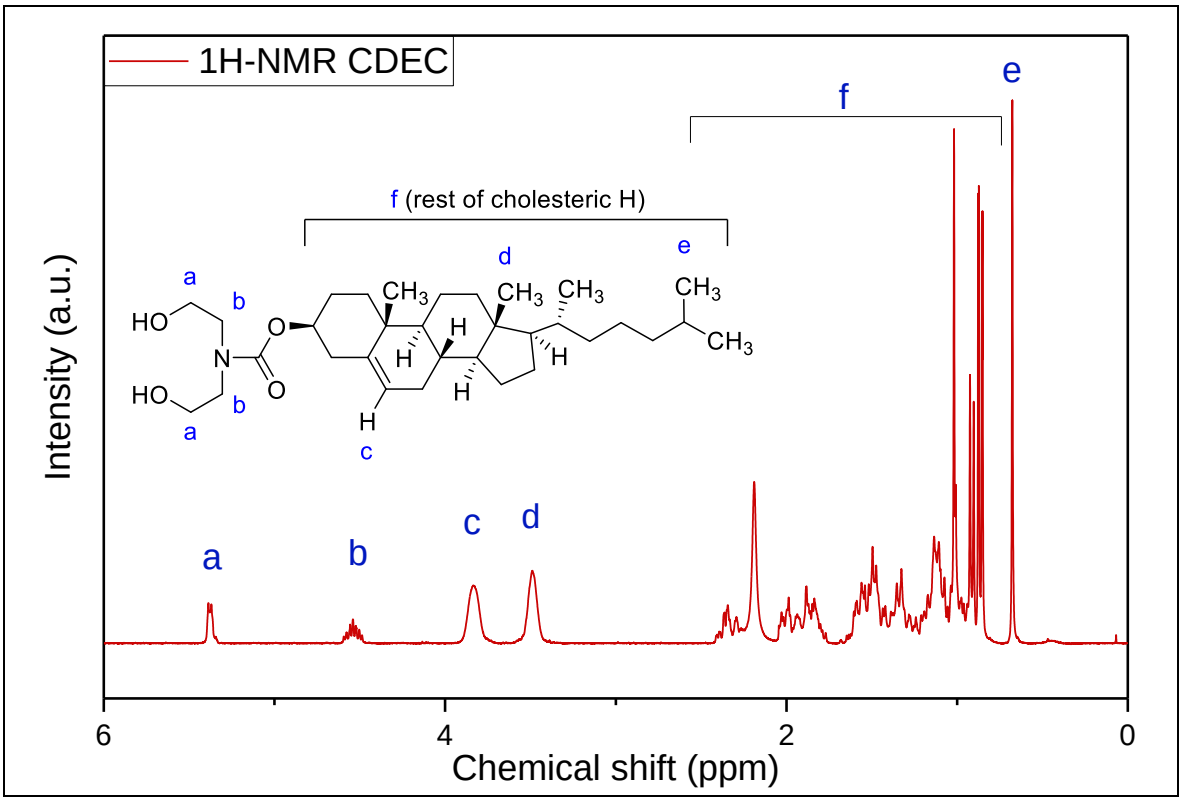

Figure 12. CDEC 1H-NMR spectrum.

5.2. LINEAR POLYURETHANE HOMOPOLYMERS SYNTHESIS AND CHARACTERIZATION:

5.2.1. SOLUTION STEP-GROWTH SYNTHESIS OF THE LINEAR POLYURETHANE HOMOPOLYMERS:

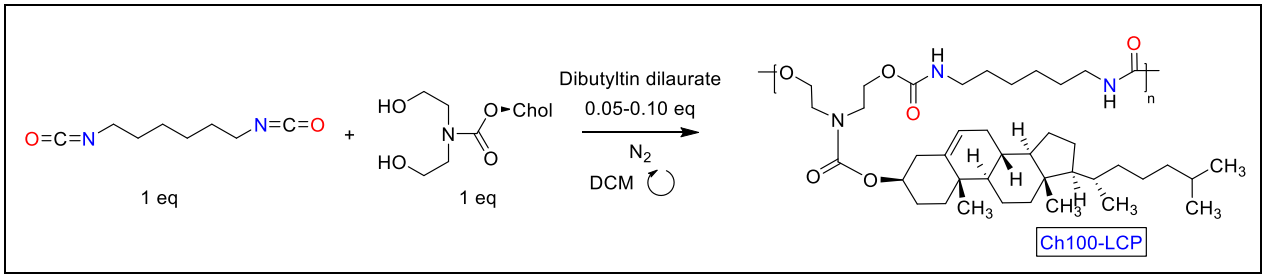

Figure 13. Simplified synthesis reaction route used for all three synthetized homopolymers: Ch100-LCP, SLP and BLP.

The same solution step-growth synthesis route [Figure 13] was followed for all linear polyurethane based homopolymers (Ch100-LCP, SLP and BLP). Since the main targets of this project were the synthesis, characterization and property analysis, an organotin compound (dibutyltin dilaurate) was chosen as catalyst due to their well-known effectiveness regardless the drawbacks entailed to them.

Besides the cholesteric monomer and the its phenyilc counterpart, the chosen diisocyanate used elaborate the polyurethane structures was hexamethylene diisocyanate (HDI). Additionally, to synthetize different copolymers (discussed in detail in section 5.3.), polypropylene glycol (PPG) of 1000Da was chosen as comonomer. The high mobility of the amorphous polyurethane segments composed of HDI and PPG_{1000} allowed to obtain polyurethanes with low glass transition temperatures, which are required to display LC behaviours at ranges far from the common degradation temperatures. Therefore a pure PPG and HDI homopolymer was synthetized to be compared with the copolymers.

In an N_2 anhydrous atmosphere, the corresponding diol quantity (CDEC/BDEC) was solubilized in near to 5 mL in a 20mL vial and stirred vigorously. The used solvent was chosen considering its capability of solubilizing all monomers, catalyst and resulting polymer (THF or DCM). Once the diols got solubilized, the hexamethylene diisocyanate was added and a sample of the stirred solution was taken as starting point for the reaction kinetics. Finally, the organotin catalyst was added (Dibutyltin dilaurate) to the reaction and the resulting mixture was stirred at room temperature taking samples periodically to follow the reaction kinetics, which were cooled at 0°C and then analyzed by FT-IR as soon as it was possible.

5.2.2. CHARACTERIZATION OF LINEAR POLYURETHANE HOMOPOLYMERS:

As expected, the obtained FTIR spectra showed the characteristic bands of the obtained cholesterol derivative monomer as well as the ones of the resultant linear polyurethanes. Those FTIR signals jointly to the different obtained NMR spectra served to confirm that the obtained products matched the structure of the desired molecules [Figure 14].

Due to the environmental humidity, all performed FTIR analyses displayed the broad O-H stretching signal near to 3400cm^{-1} making impossible to detect any hydroxyl trace. Furthermore, all N-H stretching bands at 3415cm^{-1} got overlapped inside the O-H band, the signal was only visible in the Ch100-LCP spectrum due to its higher N-H bond ratio

per polymer unit. Since all the studied compounds presented C(sp^3)-H bonds, all the spectra showed the unmistakable intense C(sp^3)-H stretching bands at 2970-2780cm^{-1}. Despite all obtained linear polyurethanes share in common a urethane group, each one showed a different wavenumber position for the C=O stretching vibration band due to the different conjugations of their carbonyl groups. Therefore, the transmittance maximums of the carboxylic bands varied between 1720cm^{-1} and 1680cm^{-1}. In addition to de carboxylic band, the carbamate groups exhibited the sigma C-N in-plane bond bends at 1540cm^{-1}. As a result of the methyl and methylene presence in all used monomers, the CH_2 symmetrical bending (scissoring) and the symmetric CH_3 bending (umbrella) were clearly visible in the spectra at 1455 cm^{-1} and 1370 cm^{-1} respectively. The carbamate groups also displayed their C-N and C-O stretching bands which showed to be merged in the frequency range comprised between 1270cm^{-1} and 1250cm^{-1}. Lastly, the SLP sample showed the polyether C-O antisymmetric stretching band that could be seen near to 1110cm^{-1}.

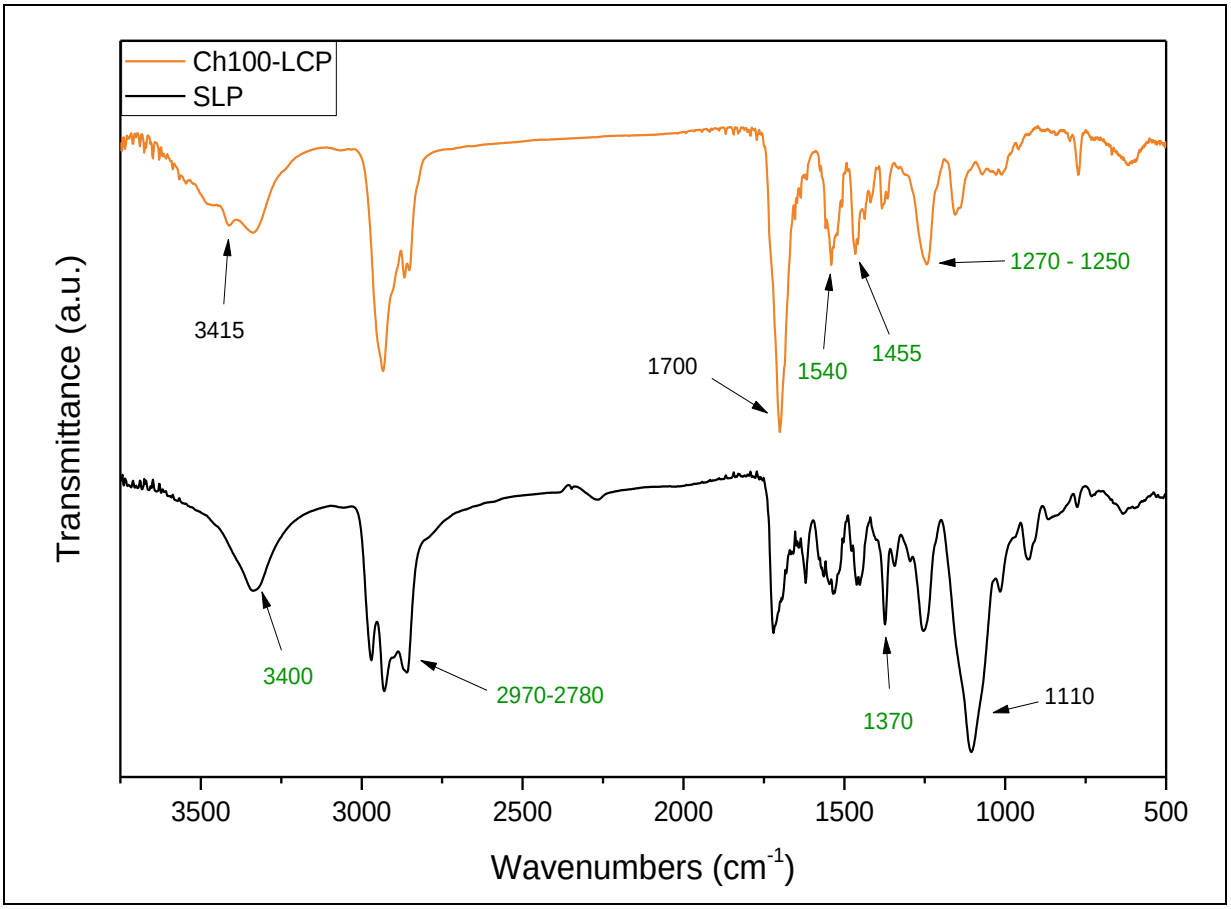

Figure 14. Ch100-LCP and SLP compared FTIR spectra. Green labels correspond to signals shared in common by all analyzed compounds.

Furthermore, the reaction kinetics of each could be followed analyzing the obtained FTIR spectra the isocyanate stretching signal at 2270cm^{-1} which disappears due to its conversion to a carbamate group [Figure 15]. Taking into account the different reactivities observed for each monomer, the selected reaction times for each polymer was determined by the results of the kinetics obtained for every reaction. Thus, the kinetics of SLP and Ch100-LCP showed a clear gap between reaction required times to reach high diisocyanate conversions that suggested that the PPG has a much higher reactivity ratio than CDEC.

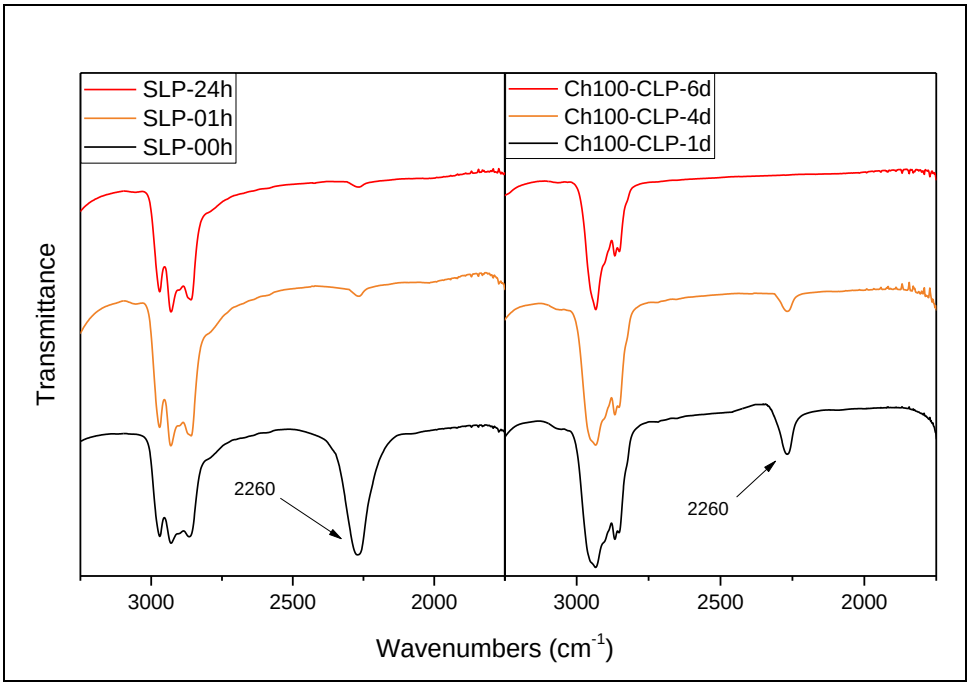

Figure 15. SLP and Ch100-LCP kinetic samples' FTIR spectra at different reaction times.

As with the previously synthetized cholesteric monomer, there was no ^{1}H-NMR nor ^{13}C-NMR characterization data of the synthetized polymeric structures. Therefore, ^{1}H-NMR analyses were performed to each product [Figure 16] to ensure that the obtained compound matched the desired chemical structure without any visible side reaction compound traces. Again, all molecule's protons were successfully assigned.

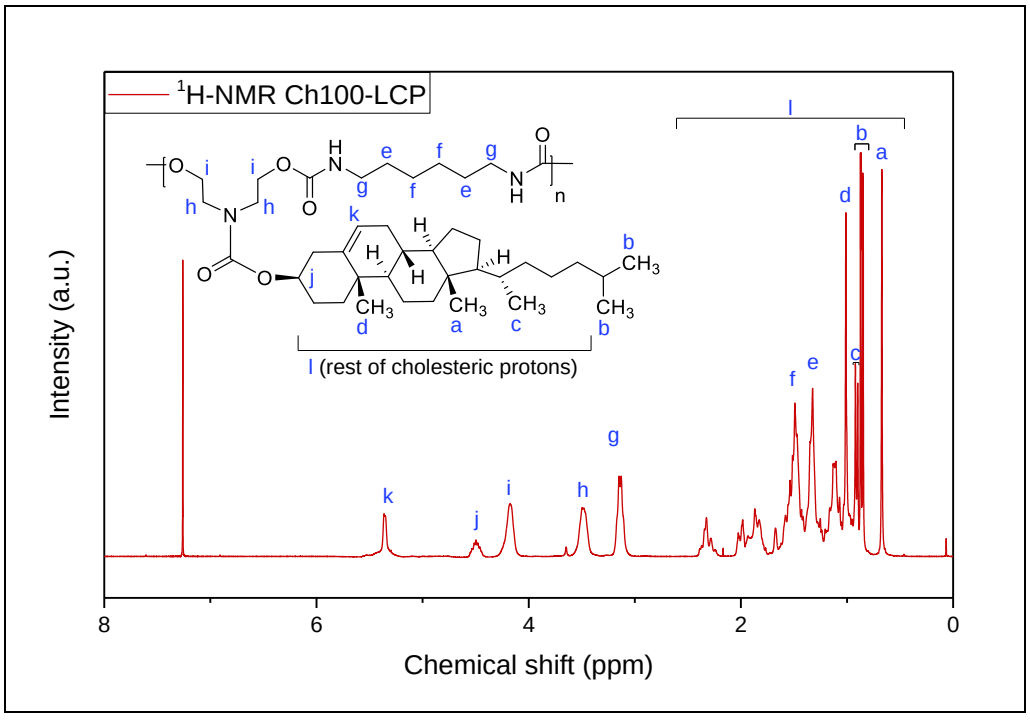

Figure 16. Ch100 ^{1}H-NMR spectrum.

In addition to FTIR analyses, both cholesterol and phenyl based polyurethanes monomer conversion could be followed qualitatively thanks to the shift of the CH_2 bonded to the oxygen atoms that reacted leading to the formation of carbamate groups. The mentioned chemical shift was detected approximately from δ = 3.8ppm to δ = 4.2ppm for Ch100 and BLP polymer samples [Figure 17].

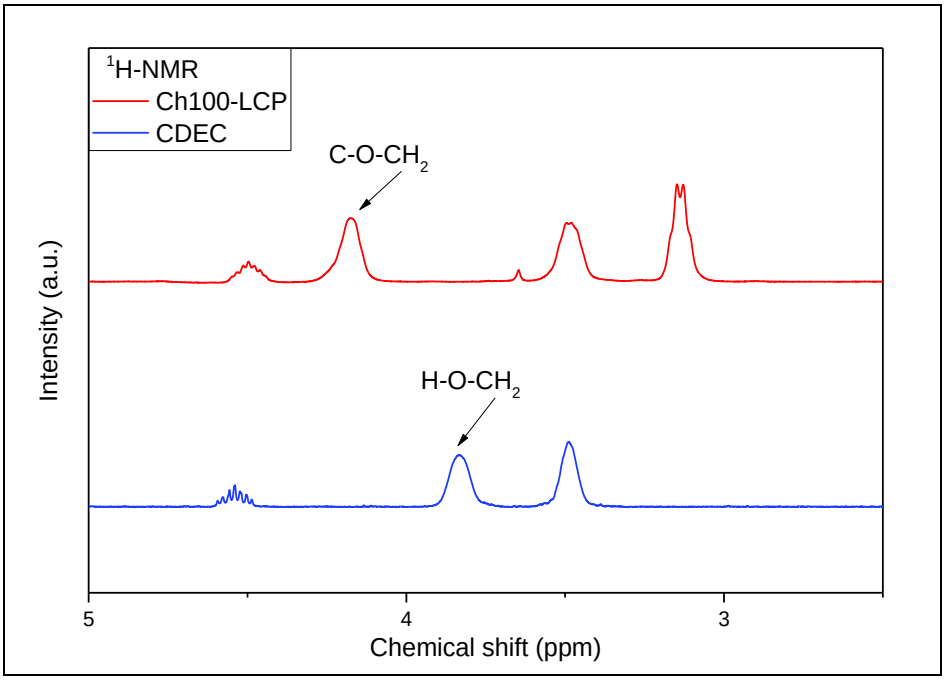

Figure 17. CDEC monomer and Ch100-LCP ^{1}H-NMR spectra at the ppm ranges at where chemical shift occurs.

The obtained results for all homopolymerization reactions suggested that the hexamethylene diisocyanate reacted properly with all three diols giving three different homopolymers as products. Thus, to obtain different cholesterol based polyurethanes with modified properties, several copolymerization reactions with distinct CDEC and PPG_{1000} ratios were performed.

5.3. SYNTHESIS AND CHARACTERIZATION OF LINEAR POLYURETHANE COPOLYMERS:

5.3.1. SOLUTION STEP-GROWTH SYNTHESIS OF LINEAR POLYURETHANE COPOLYMERS:

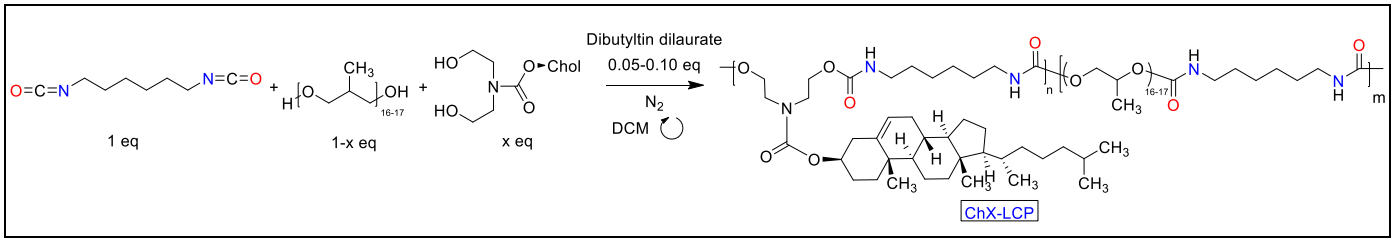

Figure 18. Simplified ChX-LCP copolymer synthesis reaction.

The route followed to obtain all copolymers [Figure 18] was the same as the one used for the previously synthetized homopolymers, commencing from solubilizing together the mix of CDEC and PPG at the corresponding molar ratios [Table 2] and then following the exact same path.

Table 2. Number of comonomers and equivalents selected for each cholesterol based polyurethane synthesis.

Polymer label	Components	Number of equivalents of each reaction component			
		HDI	PPG	CDEC	DBTDL
Ch10-LCP	3	1.0	0.9	0.1	0.05
Ch20-LCP	3	1.0	0.8	0.2	0.05
Ch50-LCP	3	1.0	0.5	0.5	0.05
Ch80-LCP	3	1.0	0.2	0.8	0.10
Ch90-LCP	3	1.0	0.1	0.9	0.10
Ch100-LCP	2	1.0	-	1.0	0.10

5.1.1. CHARACTERIZATION OF LINEAR POLYURETHANE COPOLYMERS:

Since all synthetized copolymers are the result of the combination of both SLP and Ch100-LCP composing monomers, the recorded FTIR spectra displayed the bands registered for both mentioned compounds' spectra joined together [Figure 19]. The main difference between the cholesterol based homopolymer and copolymers was the polyether C-O antisymmetric stretching band detected near to 1110cm^{-1}.

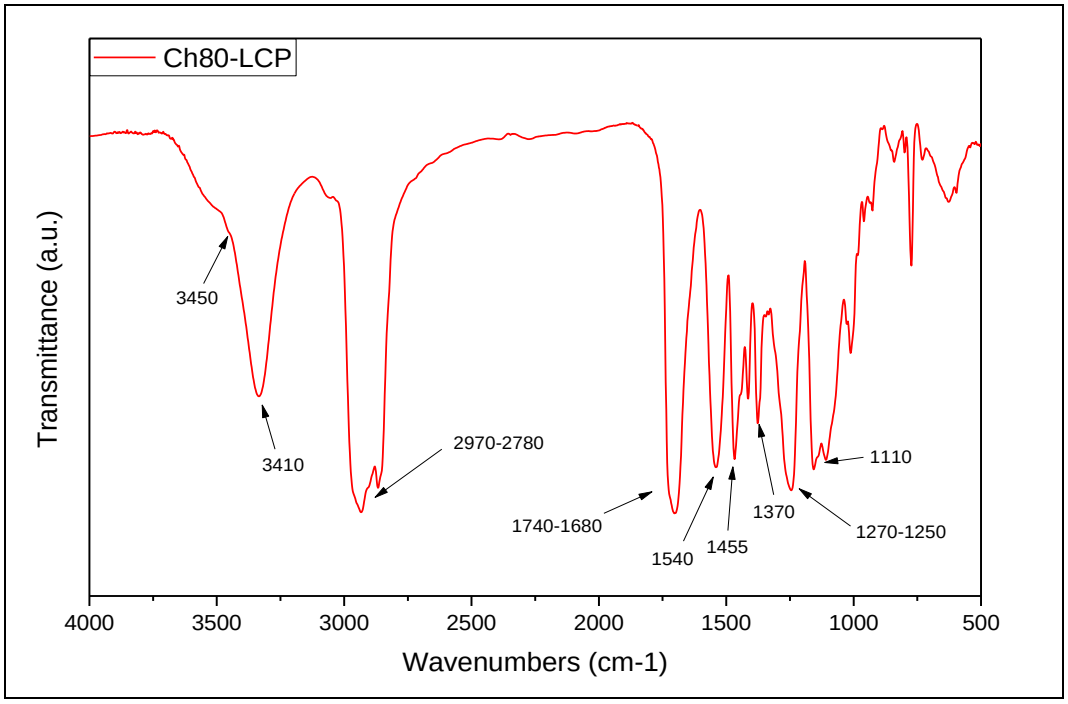

Figure 19. Ch80-LCP FTIR spectra where all the mentioned signals detected for Ch100-LCP and SLP can be clearly-seen.

Therefore, ^{1}H-NMR analyses were performed to the products [Figure 20] to ensure that the obtained compound matched the desired chemical structure without any visible side reaction compound traces.

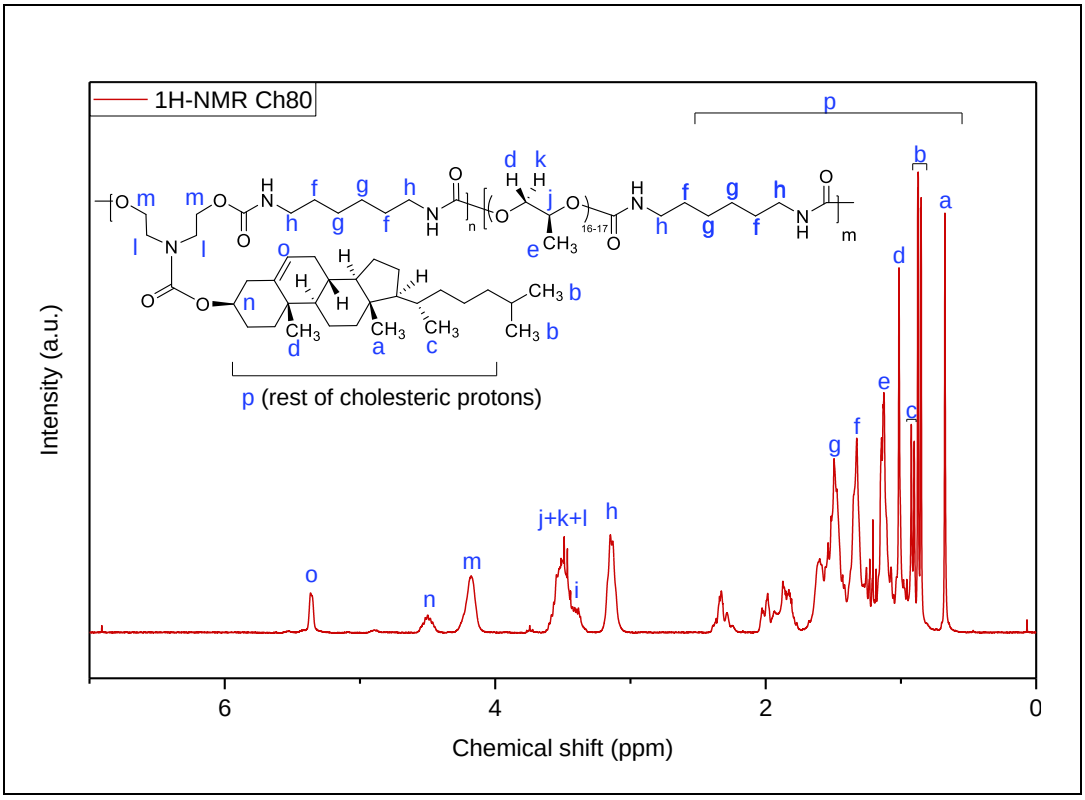

Figure 20. Ch80-LCP ^{1}H-NMR spectrum.

As with Ch100-LCP, all cholesterol based copolymer conversions were qualitatively followed by analyzing the same methylene signals' shift from "δ = 3.83" to "δ = 4.18".

Moreover, it was possible to calculate the cholesterol ratio of all LCPs by analyzing the respective ^{1}H-NMR peaks of the HDI residues' CH_2 that were bonded to the carbamate nitrogen atoms "δ = 3.14 (d, 2H, J = 0.02)" and the cholesteryl groups' most shielded CH_3 "δ = 0.68 (s, 3H)" [Figure 21].

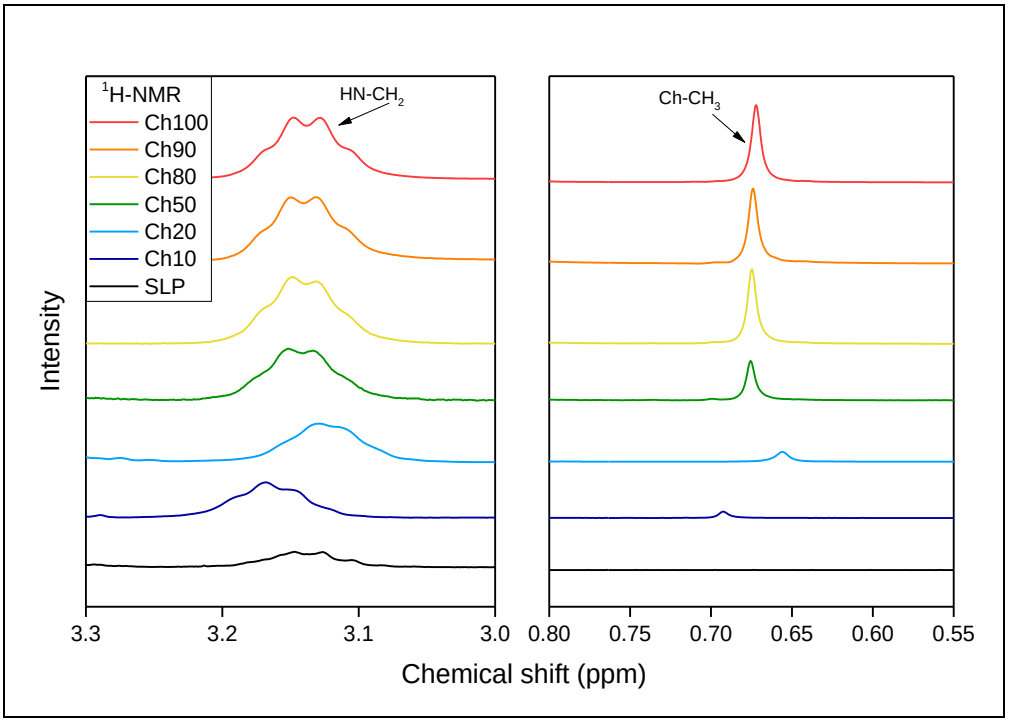

Figure 21. Enhanced ChX-LCP and SLP ^{1}H-NMR spectra regions between 3.3-3.0 and 0.80-0.55 ppm.

The mentioned peaks' integrals (I) were used to calculate the actual CDEC/HDI residue ratio setting for each polymer the HDI peak as reference [Table 3].

Table 3. Measured integral values for all synthetized cholesterol based polymers and their resulting CDEC/HADI ratios.

Compound	HDI Peak Integral	CDEC Peak Integral	Monomer ratio
Ch10-LCP	4.00	0.42	0.140
Ch20-LCP	4.00	0.76	0.253
Ch50-LCP	4.00	1.58	0.527
Ch80-LCP	4.00	2.49	0.830
Ch90-LCP	4.00	2.75	0.917
Ch100-LCP	4.00	2.99	0.997

All calculated monomer ratios of matched the CDEC/PPG_{1000} ratios chosen to be synthetized in this project, validating the proposed composition for every copolymer.

5.4. SEC-GPC ANALYSIS OF CH100/90-LCP:

As mentioned before, the CDEC monomer samples required longer reaction times. Therefore, a size exclusion chromatography (SEC-GPC) test was carried out to the polymers with the highest CDEC content [Figure 22] to verify if those compounds could be considered as polymers by analyzing their average molar mass.

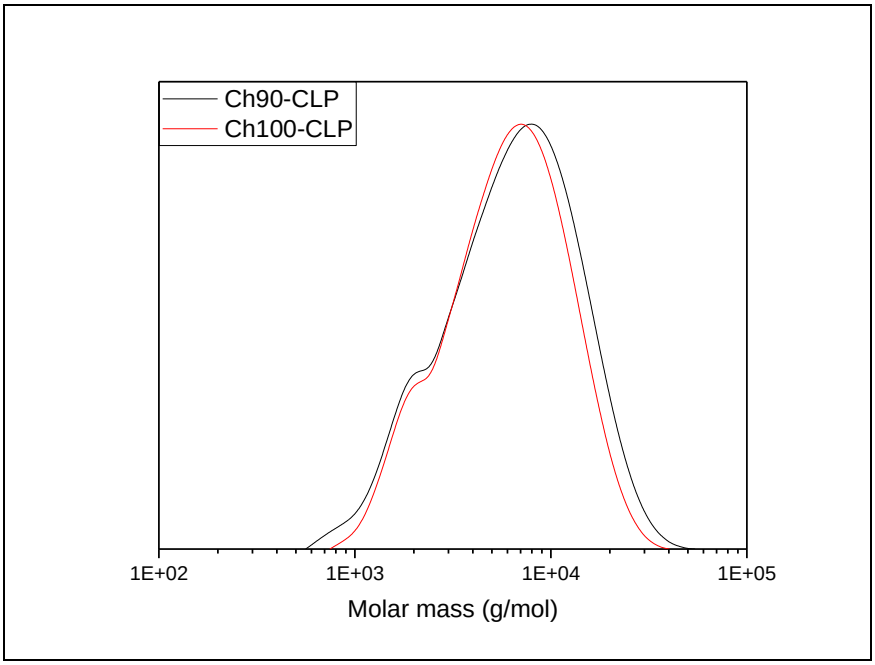

Figure 22. Ch100-LCP and Ch90-LCP molar mass distribution graphs.

Table 4. Number and weight average molar masses obtained on the SEC-GPC analysis for Ch90-LCP and Ch100-LCP.

Compound	M_n (Da)	M_w (Da)	Đ
Ch90-LCP	4465	8099	1.81
Ch100-LCP	4550	7369	1.62

The weight average molecular masses (M_w) of both compounds Ch90-LCP and Ch100-LCP [Table 4] were high enough to be considered as low molecular weight polymers. Low molecular masses are common in solution step-growth polymerizations, since a well-balanced stoichiometric quantity of every comonomer is required in order to get high polymerization degrees according to Carothers' equation [1]. Were (r) stands for the stoichiometric ratio of the reactants and (p) for the reaction conversion value.

$$\bar{X}_n = \frac{1+r}{1+r-2rp} \qquad [1]$$

5.5. THERMAL CHARACTERIZATION OF LINEAR POLYURETHANES:

Different TGA analyses were carried out to different cholesterol based compounds to study their thermal stability in order to perform DSC analysis under a specific range of temperatures without degradation risk. The degradation temperatures (T_d) were assigned for a 5% of mass loss for every compound.

5.5.1. TGA ANALYSIS OF CDEC AND Ch100/50-LCP:

As can be observed in [Figure 23] the lower T_d obtained for the cholesterol based compared to the Td obtained for Ch50-LCP and C100-LCP respectively, indicates a lower thermal stability due to the alcohol functionalities or either the lower molar mass. In addition to that, the similar T_d observed for Ch50-LCP and Ch100-LCP lead to the conclusion that the responsible to the thermal degradation is likely to be the CDEC residue.

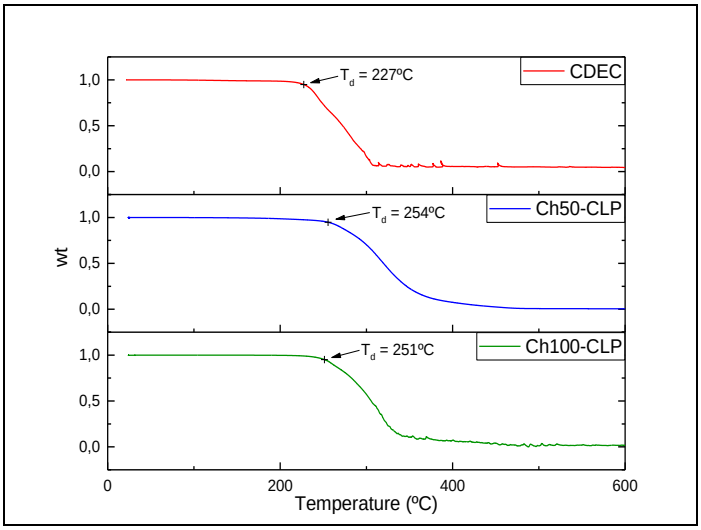

Figure 23. Ch100-LCP, Ch50-LCP and CDEC TGA thermograms.

5.5.2. DSC ANALYSIS OF LINEAR POLYURETHANE HOMOPOLYMERS AND COPOLYMERS:

Once determined by TGA analysis the T_d for different compounds, several DSC analyses were carried out in order to study the thermal behaviour of every sample with the temperature limits set at least 25°C bellow the observed T_d. All LCPs were studied from -80°C to 215°C at a 10°C/min rate [Figure***]. Analogously, melting process occurred in the first heating is visibly different to the process observed in the second heating as occurred with the CDEC sample.

The Ch90-LCP's thermogram [Figure 24] first heating scan displays a heat flow increasing rate discontinuity that takes place between 20 – 57°C. Two intense endothermic signals can be observed between 90 – 125°C and 159 – 201°C, where the scan's shape makes it possible to exist an overlapped exothermic signal between the mentioned tendency change and the first intense endothermic process. At the following first cooling scan few thermal phenomena can be observed, only a significantly weaker exothermic signal at 180 – 145°C and a less intense heat flow rate changes

63 – 20°C. Homologously, only a heat flow rate increase between 37 – 66°C and an endothermic signal 151 – 203°C can be seen in the second heating scan.

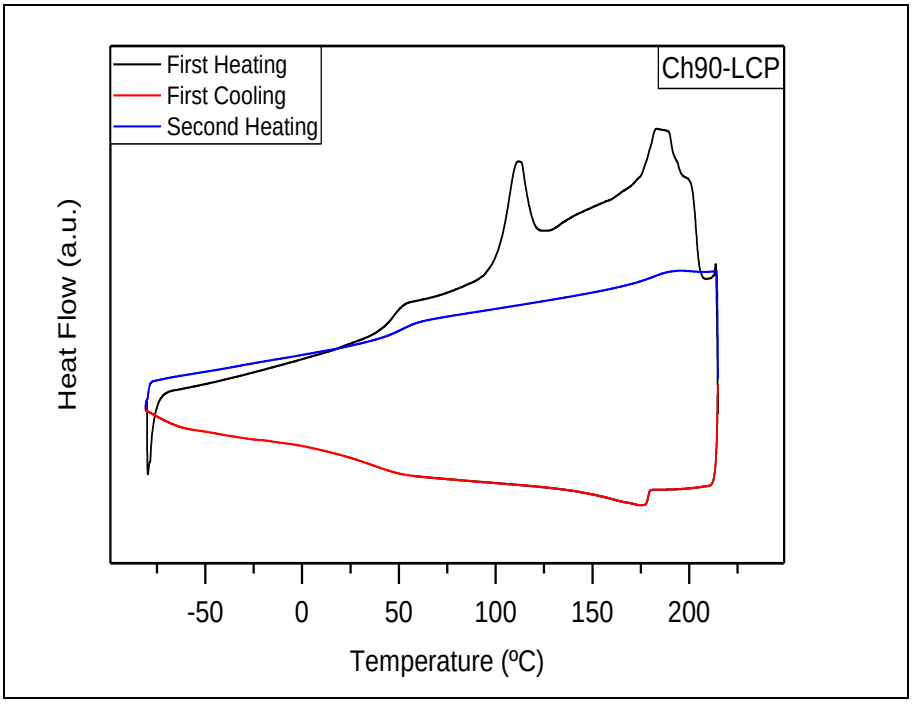

Figure 24. Ch90-LCP DSC thermogram (Exo Down).

All heat flow rate variations described before can be interpreted as the glass transition phenomena produced in the polymers amorphous regions due to specific heat capacity variations, since all of them can be seen on every scan at the same approximate temperature ranges. The overlapped endothermic process occurred in the first heating scan could be due to a cold crystallization process allowed once the glass transition temperature is surpassed. At higher temperatures, the first intense endothermic signal (90 – 125°C) can be assigned to a liquid crystalline mesophase formation from the previous crystalline structure which seems like is not reversible since this signal cannot be seen on ulterior scans. Finally, the last endothermic signal (159 – 201°C) can be assigned to a mesophase – isotropic transition. On both first cooling and second heating scans, only the glass transition and mesophase – isotropic transitions seem to appear. The absence of the crystal melting peak (leading to the liquid crystalline mesophase formation) indicates that no crystals are formed when the system is cooled down from the melt at 10 °C/min. Note, however, that the precipitation of the polymer from the solution induces the formation of crystals (as revealed in the first heating scan). Additionally, the measured mesophase-isotropic transition enthalpy values for both first cooling and second heating processes are close enough to consider that the samples did not get degraded during the analyses.

The aim is to investigate the liquid crystalline features of the material, as such, special attention will be paid to the high-temperature endothermic process, i.e. the mesofase-to-isotropic transition. First of all, in order to ensure that those reversible signals (at 159 – 201°C in the case of Ch90-LCP) are a consequence of a the pending mesogenic group, the Ch100-LCP sample was compared with a blank linear polyurethane (BLP) composed of an identical polymeric chain but with a benzylic group pending from the backbone instead of the cholesteric functionality. The absence of any endothermic features in the second heatings of the BLP [Figure 25] proves that the detected signals in Ch80, Ch90 and Ch100 LCPs are due to the mesogenic unit.

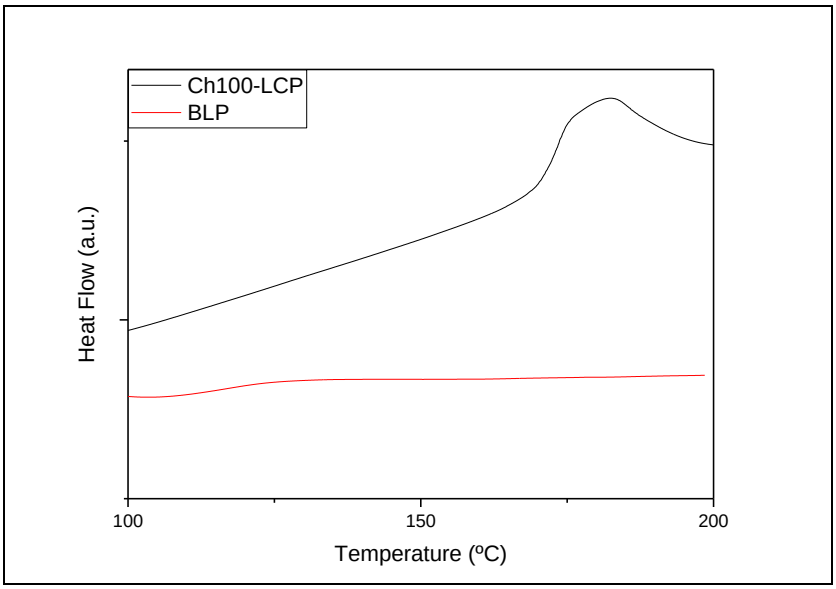

Figure 25. Ch100-LCP and BLP second heating DSC results near the detected mesophase-isotropic temperature ranges for ChX-LCPs (Exo Down).

The mesophase-isotropic transition processes [Figure 26] could only be observed in Ch80-LCP, Ch90-LCP and Ch100-LCP. Interestingly, the temperature of the phase transition seems not to depend strongly on the composition of the copolymer (for this composition range). However, the endothermic peaks become broader as the cholesterol content in the polymer decreases. The second unit in the polymeric chain alters the formed copolymer sequencing structures and the enhancing the backbone mobility, resulting this in a larger heterogeneity of the formed mesophase domains.

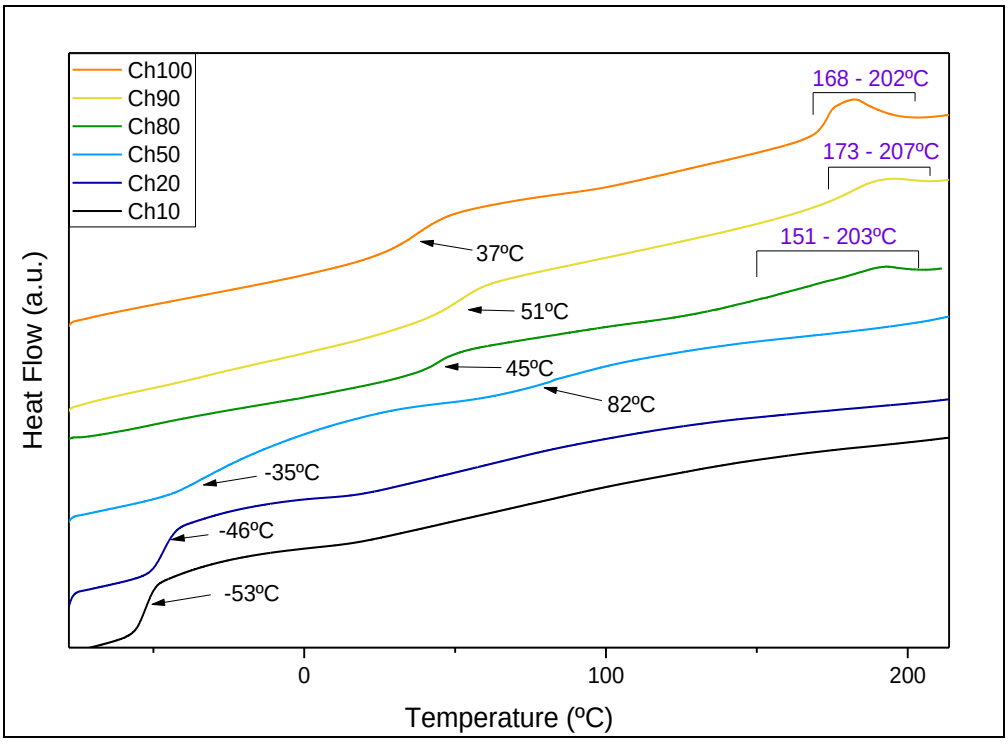

Figure 26. All ChX-LCP DSC second heatings thermograms (Exo Down).The Glass-transition temperatures are labeled in black and fusion ranges in blue.

Besides the mesophase transition, two different glass transition processes can be observed. The first glass transition temperature (detected between -53°C and -35°C depending on the polymer structure) decreases along with the cholesterol content on the polymer, which suggests that this thermal behaviour is due to the polypropylene glycol residue in the polymeric backbone. The second Tg (detected between 37°C and 82°C) only appears in LCPs with high cholesterol content, suggesting that this glass transition is related to the resulting polymeric backbone of the reaction between CDEC and HDI. As both different Tg can be observed separately in polymers with different cholesterol ratios (in the case of Ch50-LCP sample, both of them are visible), a polymer with a certain degree of blocky structure can be proposed.

5.6. POM ANALYSIS OF CH100/90/80-LCP:

5.6.1. POM DATA ADQUISITION PROCEDURE:

Within the hot stage, the polymer pieces were sandwiched between a glass slide and glass coverslip. The coverslip was placed gently over the molten polymer samples in order not to reduce excessively the sample thickness. To determine the phase transition temperatures, the samples were heated at a constant rate while images and spectra (in visible wavelength region) were simultaneously collected. Under a nitrogen atmosphere, a heating rate of 10°C/min was applied and the experiments were programmed to record the mean values of three consecutive spectra every 5°C/30s. To study the materials birefringence, the transmitted intensity at each temperature spectra was then integrated between the suitable wavelength range (480 to 700 nm) to obtain the value of the total intensity transmitted through the materials, as can be seen in the example given in [Figure 27]. Additionally, photographs of the samples were taken every 5°C to have a visual evidence to be compared with the collected data.

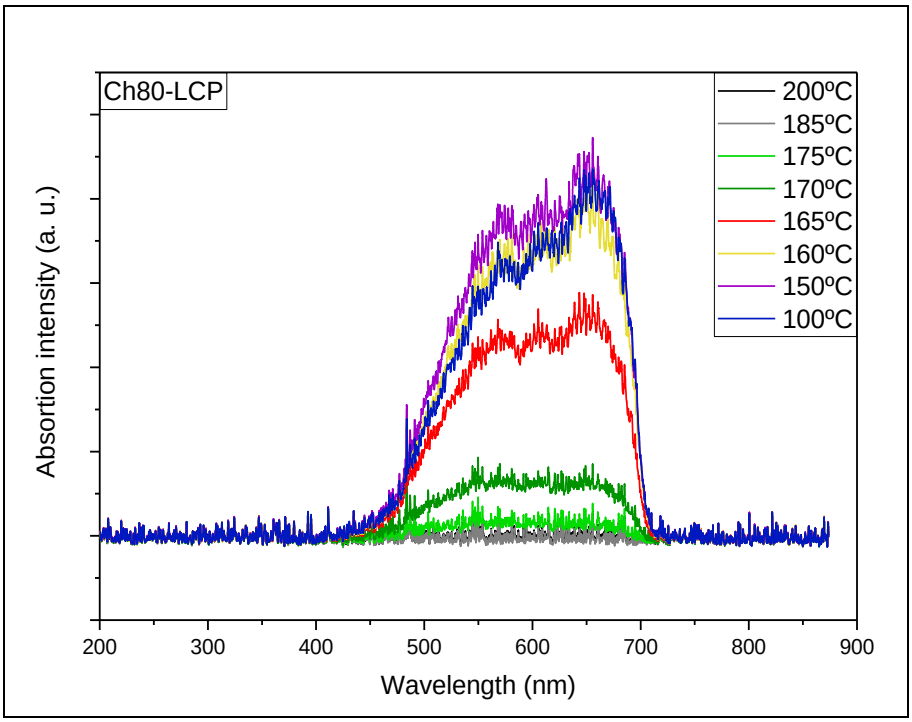

Figure 27. Ch80-LCP first cooling bright field absorption spectra at different temperatures.

Since the polarized light beam reaches the spectrometer because of the interaction with the birefringent liquid and anisotropic crystal phases, the total intensity of the collected spectra is directly related to the relative amount of mesophase at each temperature. Therefore, normalized the integral of the transmitted light intensity (Γ) can be considered as a conversion index for the different phase transitions. Hence, Γ holds the unit value when the material presents most the birefringent state and on the other hand, Γ turns out to be null for all non-birefringent phases such as the isotropic state. Consequently, the phase transition temperatures ranges can be described as the temperatures at which the Γ tendency fluctuates undergoing through an acceleration and deceleration process due the

birefringence variations associated to phase transitions. These results can be easily observed representing the $d\Gamma/dT$ function where the transition ranges appear like a peak in the function where the minimum value corresponds to the inflection point at which the variation holds it maximum speed.[10]

From all synthesized LCPs only Ch80, Ch90 and Ch100 displayed a liquid crystal behaviour, thus several POM experiments were conducted to study the thermal behaviour of those three compounds on first cooling and second heating processes.

5.6.2. Ch100/90/80-LCP POM COOLING PROCESS DATA ANALYSIS:

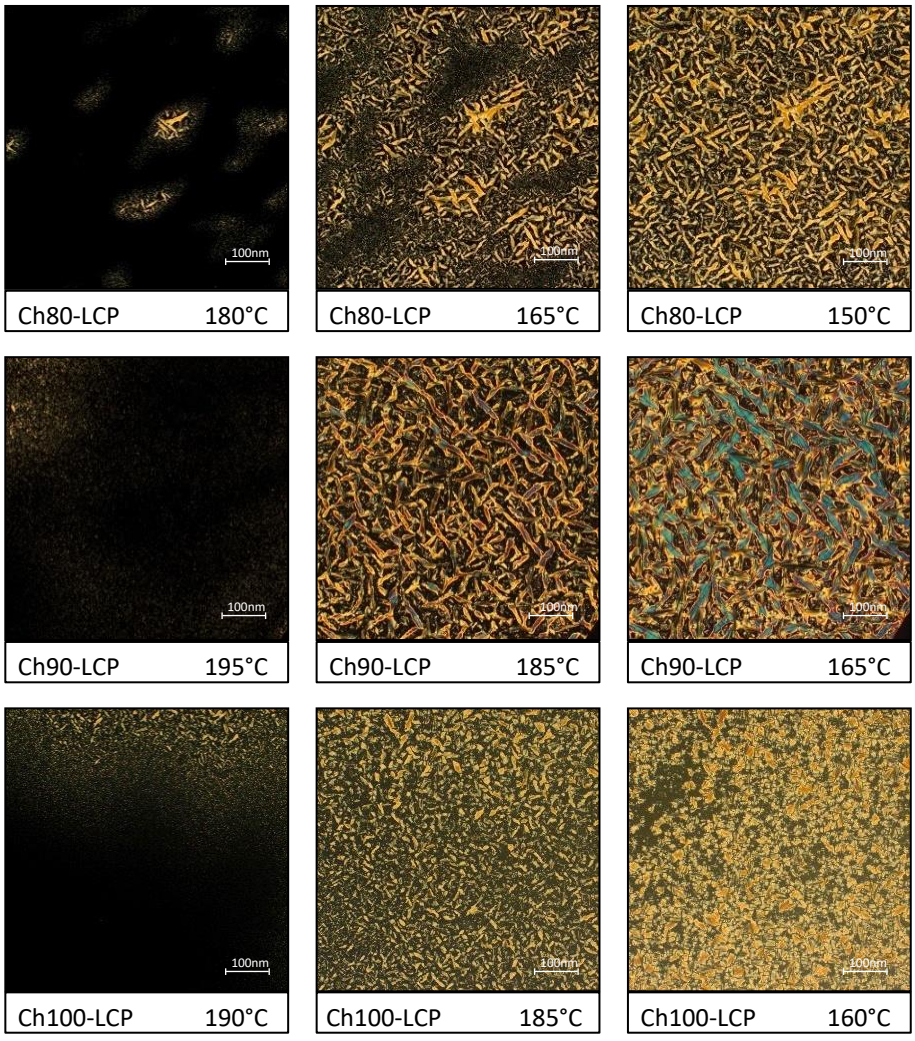

Figure 28. Ch100-LCP, Ch90-LCP and Ch80-LCP pictures taken during the isotropic – mesophase transition processes at different temperatures.

The registered data for all cooling processes [Figure 29] started at a temperature of 215°C from the isotropic state and finished at 100°C on a solid crystalline state. All three LCPs displayed the phase transition temperature pattern registered in the DSC experiments.

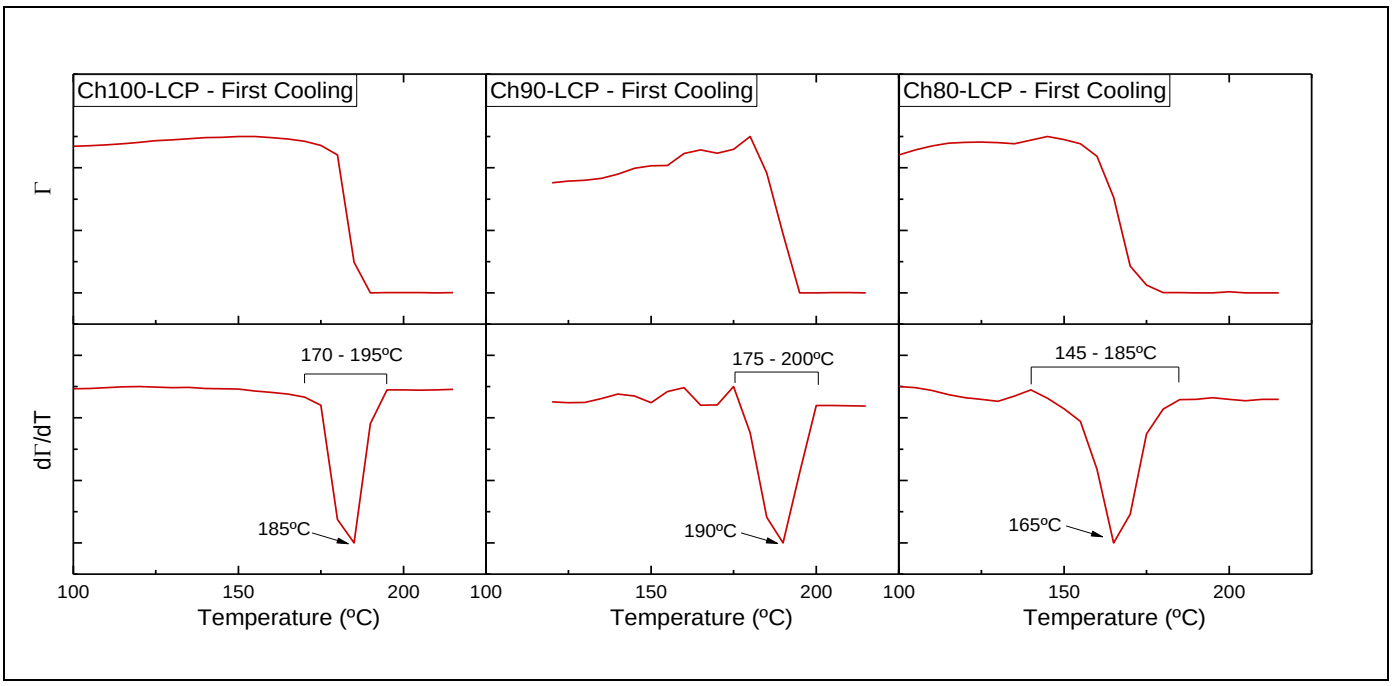

Figure 29. Ch100-LCP, Ch90-LCP and Ch80-LCP POM fist cooling Γ and $d\Gamma/dT$ results as temperature function calculated from the recorded spectra.

Compared to the heating processes discussed below [Figure 31], the observed narrower transition temperature ranges [Tables 5 – 6] are due to the kinetic restriction associated to the nucleation process required to the growth of crystalline structures. In order to nucleate, the material requires a lower energy state to be able to start self-organizing its molecules, leading to a new thermodynamic phase. Immediately upon the nucleation process takes place, the liquid crystal growth immediately spreads leading to the liquid crystal mesophase [Figure 28].

Table 5. Ch100-LCP, Ch90-LCP and Ch80-LCP first cooling mesophase-isotropic transition ranges and maximum speed transition temperatures detected by POM.

Compound	Phase transition range (°C)	Phase transition maximum (°C)
Ch100-LCP	170 – 195	185
Ch90-LCP	175 – 200	190
Ch80-LCP	145 – 185	165

5.6.3. Ch100/90/80-LCP POM HEATING PROCESS DATA ANALYSIS:

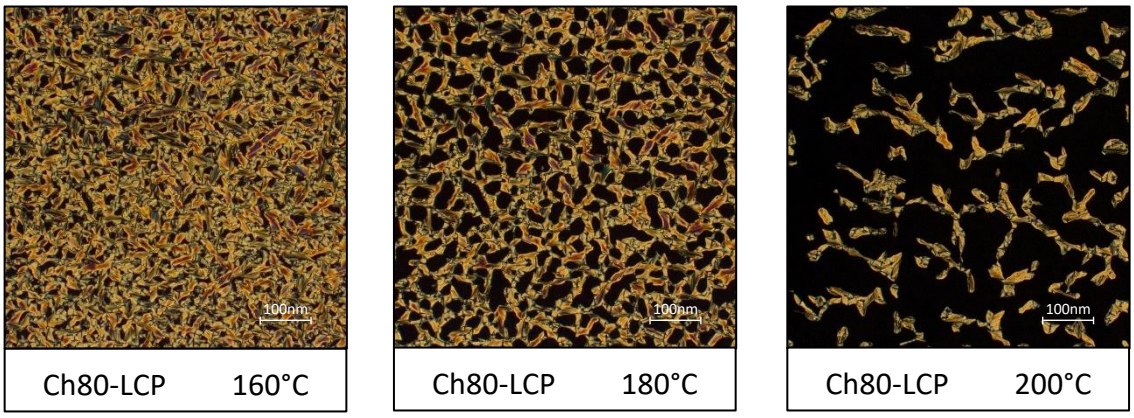

Figure 30. Ch80-LCP pictures taken during the mesophase – isotropic transition process at different temperatures.

As expected, the mesophase-isotropic transition beginning [Figure 31] of each compound was detected at the temperatures at which the phase transition ended in the respective cooling processes. As soon as the required temperatures were reached, the samples commenced to randomly grow isotropic spots [Figure 30] until reaching the total phase transition. All recorded mesophase-isotropic transition end temperatures were above the initial crystal growth temperatures detected on each cooling process.

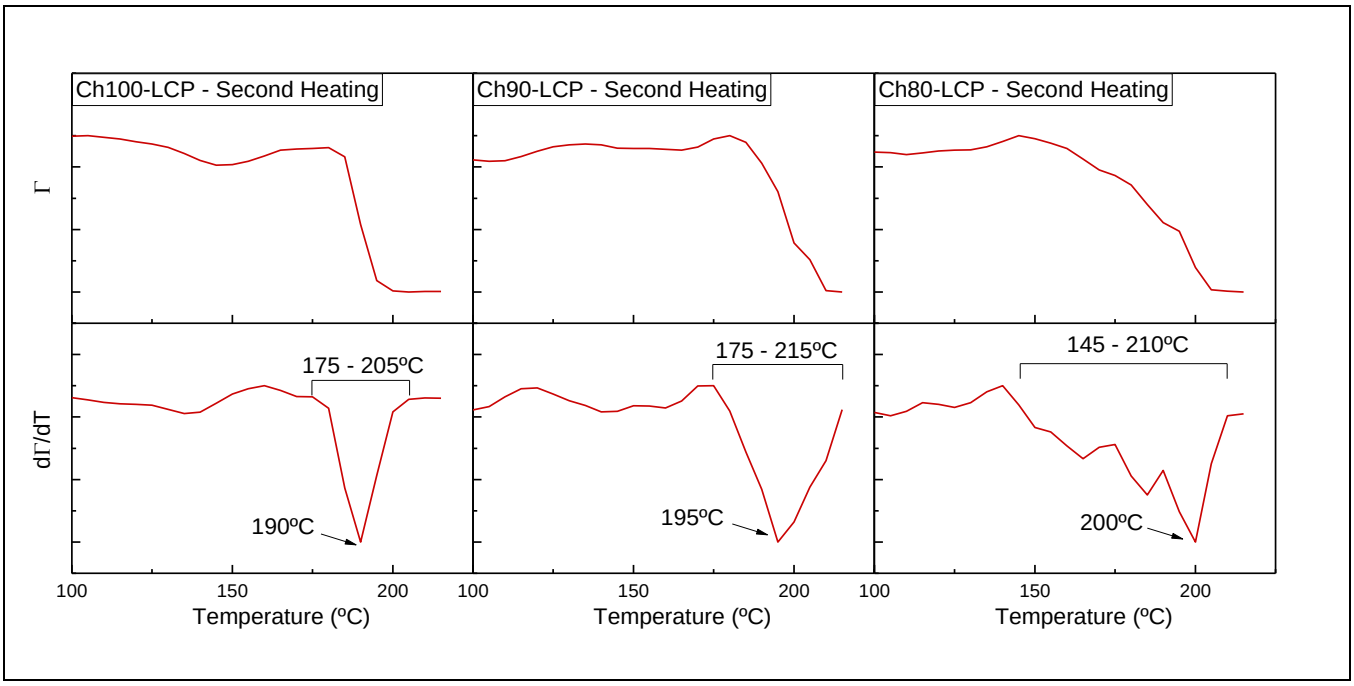

Figure 31. Ch100-LCP, Ch90-LCP and Ch80-LCP POM second heating Γ and dΓ/dT results as temperature function calculated from the recorded spectra.

As consequence of the lack of the kinetic restriction imposed by the nucleation mechanism, all samples displayed the mesophase-isotropic transition equilibrium at its full temperature ranges. However, the random positioning of the continuously growing isotropic areas [Figure 30], in addition to the flowing of the liquid material, enhanced the experimental error of every recorded spectra. Even so, the collected data match the expected behaviour compared to the results of the second heating process DSC thermograms.

5.6.4. POM Ch100/90/80-LCP RESULTS AND DISCUSSION:

As shown in [Table 6] , the obtained results for all three LCPs match approximately each samples' individual behaviour detected in the previously conducted DSC analyses, where the mesophase-isotropic transitions wideness was proven to be affected by the cholesterol content.

Table 6. Ch100-LCP, Ch90-LCP and Ch80-LCP mesophase-isotropic transition temperature maximum's and ranges at the POM and DSC in second heating processes.

Compound	POM phase transition maximum (°C)	DSC phase transition maximum (°C)	POM phase transition range (°C)	DSC phase transition range (°C)
Ch100-LCP	190	182	175 – 205	168 – 202
Ch90-LCP	195	192	175 – 215	163 – 207
Ch80-LCP	200	193	145 – 210	151 – 203

5.7. CH100-LCP X-RAY SCATTERING ANALYSIS:

In order to understand the thermal behaviours seen in POM and DSC experiments, a Ch100-LCP sample was analyzed by wide angle X-Ray scattering. The obtained results allowed us to gather more information about the molecular arrangement transitions during heating and cooling processes.[11]

5.7.1. WAXS ANALYSIS OF Ch100-LCP:

In the first heating scan, at low temperatures (between 10 – 110°C to be precise), an intense Bragg reflection can be observed at 14.5 nm^{-1} in addition to the amorphous halo [Figure 32]. At 120°C the signal almost disappears inside the amorphous halo. This peak can be associated with the polymer crystals present in the as-synthesized (and annealed during the drying process) material.

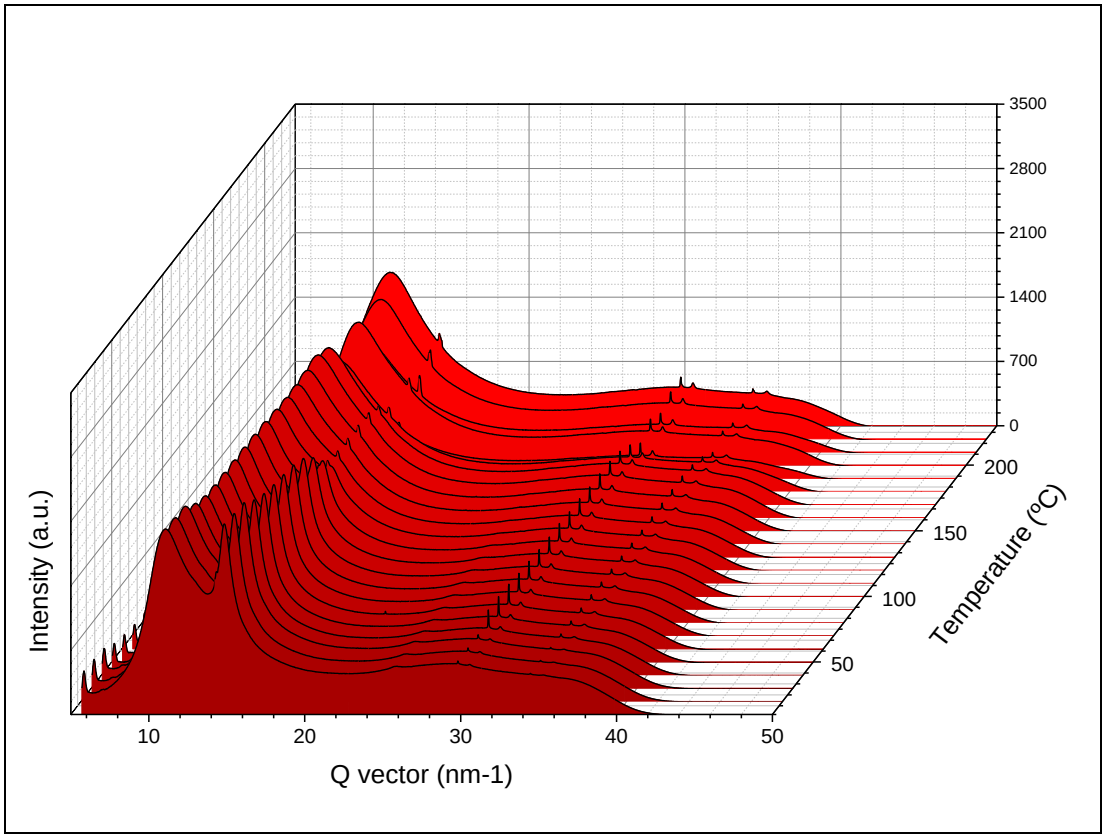

Figure 32. First heating process WAXS results of Ch100-LCP.

This phenomenon could serve to give an explanation to why the following cooling process [Figure 33] only displays a more intense diffuse scattering halo at high temperatures. Which intensity decreases along with the temperature within the isotropic – mesophase transition temperature range detected on previous analyses without any fluctuation. The absence of the mentioned Bragg refraction signal intensity increase at 14.5 nm^{-1} matches the thermal behaviour seen in previous DSC experiments, where there was no evidence of other crystallization processes besides the formation of the liquid crystal phase.

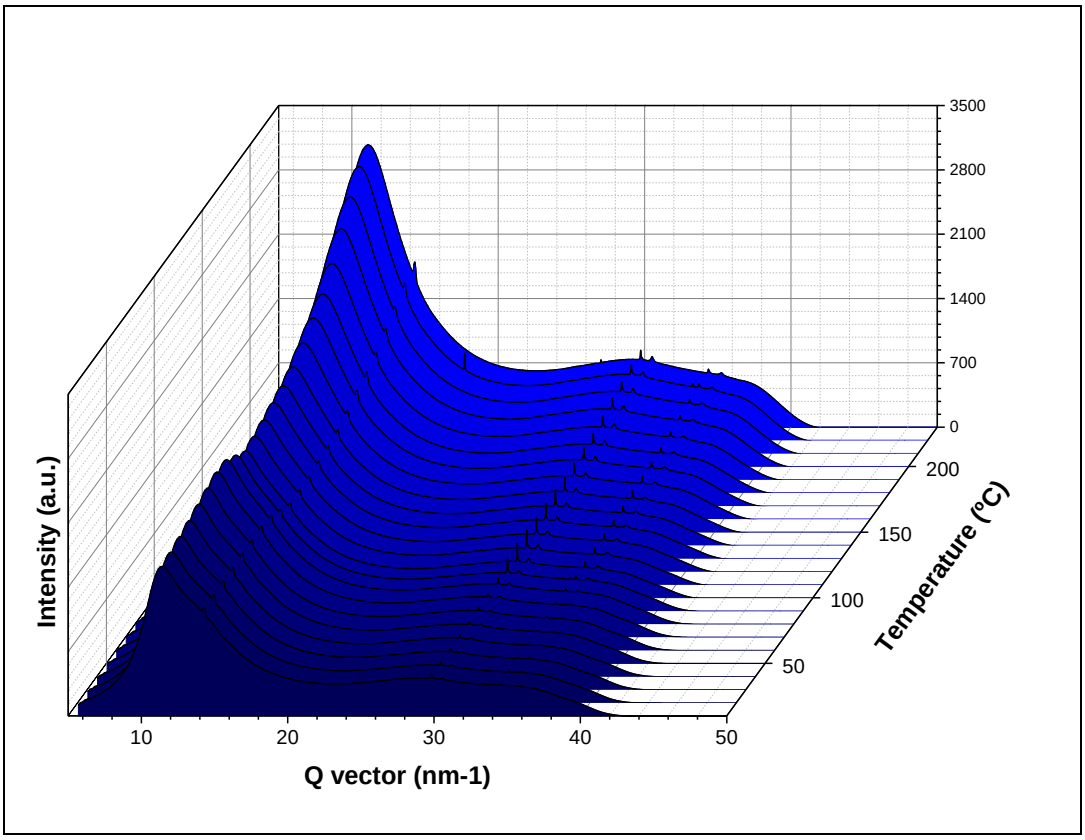

Figure 33. First cooling process WAXS results of Ch100-LCP.

6. CONCLUSIONS

Considering the obtained results, two main conclusions can be drawn. On the one hand, the conducted research for this study allowed to synthetize a new class of cholesterol based liquid crystal polymers with potential applications in biotechnology, which were successfully synthetized and characterized by a combination of different spectroscopic techniques fulfilling the objectives of the first part of the project. On the other hand, the second part's objectives were achieved since liquid crystalline behaviour was proven and profitably studied by thermal and spectroscopic analyses.

On the first part, the synthetized CDEC monomer was properly characterized and succeeded as a suitable method to conjugate the cholesteric functionalities in a polyurethane structure, stable at the temperatures at which the liquid crystalline behaviour occurs. The following solution step-growth synthesis led successfully to the desired side-chain cholesterol based polyurethanes, which structures were consequently elucidated by NMR and FTIR techniques. The qualitative analysis of the reaction kinetics allowed to confirm that the polymerization reactions were completed, regardless the different relativities detected for the CDEC and PPG in the copolymerization processes. However, the results shown by SEC-GPC analyses indicated that the obtained polymers molar masses were not as high as expected. Nevertheless, the characterization by DSC, POM and X-ray scattering experiments concluded that the polymers matched the expected behaviour attributed to this kind of compounds despite the meager molar masses.

On the second part, once the objective of obtaining a polymer able to present a liquid crystalline behaviour was achieved, consequent DSC, POM and WAXS analyses were performed in order to analyze this novel materials' properties. The gathered results showed how the as-synthetized polymers presented a crystalline structure that was irreversibly lost once the samples got molten into the liquid crystal phase. Nonetheless, the resulting mesophase did present reversible transitions into solid crystalline and liquid isotropic phases. Furthermore, the recrystallized structures (bellow 150°C) looked like a fully grown version of the shapes displayed by the mesophases. This similarity detected by POM could be the explanation to why the solid crystalline – liquid crystalline transitions could not be detected by DSC, since liquid crystal phase structures share the molecules' ordering pattern with the solid state with only slight conformational variations. DSC data also proved that low cholesterol content polymers did not present a liquid crystalline behaviour. This fact leaded to the conclusion that the studied polymers require a high mesogenic content to display a liquid crystalline state. Additionally, it was concluded that the PPG content affects to the mesophase – isotropic transition equilibrium temperature range, due to the fact that PPG residues act as an in-backbone spacer with a considerable impact on the chain's mobility. Additionally, as observed by POM, the mesophases had a confluent sword-like shaped structures that could not be assigned by this technique or any other performed characterization analysis. However, the most common mesophase structure on side-chain cholesteric linear LCPs is the chiral-nematic phase. The cholesterols bulky pending hydrocarbon structure obstructs the proper alignment of this kind of polymers creating a parallel organized structure. The cholesterol chirality usually causes the nematic phase to be chiral (known as cholesteric – nematic phase). Even so, further studies are required to make a proper liquid crystalline structure assignation.

As a closure, the results obtained in this project served to deepen into the cholesterol based LCPs chemistry and to expand the knowledge about this polymer research field, breaking new grounds to new studies.

7. FURTHER WORKS:

As a follow-up of this project results, further studies about the developed LCPs should be conducted. For instance, different monomer ratios and spacers could be studied to expand the knowledge about this type of polymers and to help to get a better understanding about their thermal behaviour. It might be convenient to find the way to obtain higher molecular masses to ensure that the samples liquid crystal behaviour characteristics are due to their polymeric structures increasing the precision of the stoichiometric quantities added to the reaction medium. In addition to the obtained MAXS results, mesophase structure information could be obtained performing a small and medium angle X-ray scattering analysis, which could lead to the elucidation of the mesophase structure type.

Additionally, it could be interesting to search for an alternative synthesis path to avoid the drawbacks of organotin catalysts and the toxicity of the utilized solvents. Thus, the biocompatibility of the polymer could be improved, and the synthesis route would be closer to a greener approach. Nonetheless, the samples biocompatibility should be tested before starting a proper study of the possible biotechnological applications. If the materials proposed in this project turn out to be biocompatible, they would result worth to have their potential biotechnological applications studied. Since, as mentioned before the obtained materials surfaces could serve as a liposome anchoring hotspots and heterogeneously favored cell grow areas.

8. REFERENCES:

1. T. Scharf, Polarized light in liquid crystals and polymers, Wiley-Interscience, Hoboken, N.J, 2007. ISBN-978-0-471-74064-3.

2. J. Beeckman, Optical Engineering, 2011, 50, 081202.

3. E. Mehravar, A. Iturrospe, A. Arbe, J. M. Asua and J. R. Leiza, Polymer Chemistry, 2016, 7, 4736–4750.

4. H. Sardon, A. Pascual, D. Mecerreyes, D. Taton, H. Cramail and J. L. Hedrick, Macromolecules, 2015, 48, 3153–3165.

5. H.-W. Engels, H.-G. Pirkl, R. Albers, R. W. Albach, J. Krause, A. Hoffmann, H. Casselmann and J. Dormish, Angewandte Chemie International Edition, 2013, 52, 9422–9441.

6. R. N. Jana and J. W. Cho, Fibers and Polymers, 2009, 10, 569–575.

7. L. Hosta-Rigau, Y. Zhang, B. M. Teo, A. Postma and B. Städler, Nanoscale, 2013, 5, 89–109.

8. J. G. Betts, P. Desaix, e. Johnson, J. E. Johnson, O. Korol, D. Kruse, B. Poe, j. A. Wise, M. Womble and K. A. Young, Anatomy & Physiology, OpenStax, ISBN-10 1-947172-04-2, ISBN-13 978-1-947172-04-3. https://openstax.org/details/books/anatomy-and-physiology.

9. F. Ercole, M. R. Whittaker, J. F. Quinn and T. P. Davis, Biomacromolecules, 2015, 16, 1886–1914.

10. J. Martin, E. C. Davidson, C. Greco, W. Xu, J. H. Bannock, A. Agirre, J. de Mello, R. A. Segalman, N. Stingelin and K. C. Daoulas, Chemistry of Materials, 2018, 30, 748–761.

11. M. T. Sims, L. C. Abbott, R. M. Richardson, J. W. Goodby and J. N. Moore, Liquid Crystals, 2018, 1–1.